

Splines for Image Metamorphosis

Jorge Justiniano*

Marko Rajković*

Martin Rumpf*

August 3, 2021

Abstract

This paper investigates a variational model for splines in the image metamorphosis model for the smooth interpolation of key frames in the space of images. The original metamorphosis model is based on a simultaneous transport of image intensities and a modulation of intensities along motion trajectories and the energy functional measures the motion velocity and the material derivative of the image intensity. As in the case of cubic splines in Euclidean space where cubic splines are known to minimize the squared acceleration along the interpolation path we consider different acceleration terms to define a spline metamorphosis model. In fact, the proposed spline functional combines quadratic functionals of the Eulerian motion acceleration and of the second material derivative representing an acceleration in the change of intensities along motion paths.

Furthermore, a variational time discretization of this spline model is proposed and the convergence to a suitably relaxed time continuous model is discussed via Γ -convergence methodology. As a byproduct, this also allows to establish the existence of metamorphosis splines for given key frame images as minimizers of the continuous spline functional. An effective spatial discretization is proposed based on a finite difference discretization in space combined with a stable B-spline interpolation of deformed quantities. A variety of numerical examples demonstrates the robustness and versatility of the proposed method in applications using a variant of the iPALM algorithm for the minimization of the fully discrete energy functional¹.

1 Introduction

Image metamorphosis is a flexible model for image morphing generalizing the flow of diffeomorphism approach (cf. the textbook by Younes [You10]) and investigated extensively by Trounev, Younes and coworkers [TY05b, TY05a]. The approach is based on the minimization of a path energy functional over all regular paths connecting a pair of input images. Minimizers can be understood as geodesic paths in the space of images considered as a Riemannian manifold. The underlying metric associates a cost both to the transport of image intensities via a viscous flow and to image intensity variations along motion paths. The metamorphosis model has been extended to discrete measures [RY13], to reproducing kernel Hilbert spaces [RY16], to functional shapes [CCT18], to images on Hadamard manifolds [ENR20] and to deep feature spaces [EKP⁺21].

In this paper, we discuss a spline energy functional as a second order extension of the first order path energy. Given a set of key frames at disjoint times a spline path is given as a minimizer of the spline energy subject to the key frame interpolation constraint. In Euclidean space cubic splines $t \mapsto u(t)$ are known to be minimizers of the integral of the squared acceleration $\int_0^1 |\ddot{u}(t)|^2 dt$ due to the famous result by de Boor [dB63]. In a Riemannian context, Noakes et al. [NHP89] introduced

*Institute for Numerical Simulation, University of Bonn (name.surname@ins.uni-bonn.de)

¹This publication is an extended version of the previous conference proceeding [JRR21] presented at SSVM 2021.

Riemannian cubic splines as stationary paths of the integrated squared covariant derivative of the velocity.

Today, there is a variety of spline approaches in non-linear spaces and with applications to shape spaces. Trouné and Vialard [TV12] studied a second-order shape functional in landmark space based on an optimal control approach. Singh et al. [SVN15] introduced an optimal control method involving a functional which measures the motion acceleration in a flow of diffeomorphisms ansatz for image regression. Tahraoui and Vialard [TV19] consider a second-order variational model on the group of diffeomorphisms of the interval $[0, 1]$. They proposed a relaxed model leading to a Fisher-Rao functional, as a convex functional on the space of measures. Vialard [Via20] showed the existence of a minimizer of the Riemannian acceleration energy on the group of diffeomorphisms endowed with a right-invariant Sobolev metric of high order. Benamou et al. [BGV19] and Chen et al. [CCG18] discussed spline interpolation in the space of probability measures endowed with the Wasserstein metric. Thereby, energy splines are defined as minimizers of the action functional on Wasserstein space which involves the acceleration of measure-valued paths, sharing similarities with the spline functional in the space of images introduced in this paper. The initial computational intractability of such approaches is tackled by a relaxation based on multi-marginal optimal transport and entropic regularization. The transport problem this approach aims at solving might not have a Monge solution, which was remedied by a new method introduced by Chewi et al. [CCLG⁺21] to construct measure-valued splines, dubbed transport splines. This method additionally enjoys substantial computational advantages.

Here, we will introduce a spline energy as a generalization of the path energy in the metamorphosis model. This path energy consists of a first term measuring the dissipation caused by the Eulerian motion velocity field and a second term measuring the material derivative of the image intensities along motion lines. Our spline model introduces second order variants of both terms, i.e. involving the Eulerian motion acceleration and the weak formulation of the second order material derivative of image intensities. Furthermore, we will study a corresponding time discrete variational model, which generalizes the time discrete metamorphosis model proposed in [BER15, EKP⁺21] and we show the convergence of this time discrete model to the time continuous metamorphosis spline model in the sense of Mosco [Mos69]. As a consequence, one obtains existence of metamorphosis spline paths. Further discretizing the model in space we derive a numerical scheme to solve for fully discrete metamorphosis spline paths in the space of images.

Let us remark that the proposed spline model is not Riemannian in the sense that splines are minimizers of the squared covariant derivative of the path velocity as in [NHP89, TV19, Via20] or in [HRW18], where a related time discretization is proposed for Riemannian splines. In fact, our model separates in a physically intuitive way the Eulerian flow acceleration and the second material derivative of the image intensity, whereas the integral over the squared covariant derivative of the path velocity in the Riemannian metric would lead to an interwoven model of these different types of acceleration.

Notation. Throughout this paper, we assume that the image domain $\Omega \subset \mathbb{R}^d$ for $d \in \{2, 3\}$ is bounded and strongly Lipschitz. We use standard notation for Lebesgue and Sobolev spaces from the image domain Ω to a Banach space X , i.e. $L^p(\Omega, X)$ and $H^m(\Omega, X)$ and omit X if the space is clear from the context. The associated X norms are denoted by $\|\cdot\|_{L^p(\Omega)}$ and $\|\cdot\|_{H^m(\Omega)}$, respectively, and the seminorm in $H^m(\Omega)$ is given by $|\cdot|_{H^m(\Omega)}$, i.e.

$$|f|_{H^m(\Omega)} = \|D^m f\|_{L^2(\Omega)}, \quad \|f\|_{H^m(\Omega)}^2 = \sum_{j=0}^m |f|_{H^j(\Omega)}^2$$

for $f \in H^m(\Omega)$. We use the notation $C^{k,\alpha}(\bar{\Omega}, X)$ for Hölder spaces of order $k \geq 0$ with Hölder regularity $\alpha \in (0, 1]$ for the k -th derivatives and the corresponding (semi)norm is

$$|f|_{C^{0,\alpha}(\bar{\Omega})} = \sup_{x \neq y \in \Omega} \frac{|f(x) - f(y)|}{|x - y|^\alpha},$$

$$\|f\|_{C^{k,\alpha}(\bar{\Omega})} = \|f\|_{C^k(\bar{\Omega})} + \sum_{|\beta|=k} |D^\beta f|_{C^{0,\alpha}(\bar{\Omega})}.$$

The space $AC^p([0, 1], X)$ is the space of absolutely continuous functions with the derivative in $L^p((0, 1))$.

The symmetric part of a matrix $A \in \mathbb{R}^{d,d}$ is denoted by A^{sym} , i.e. $A^{\text{sym}} = \frac{1}{2}(A + A^\top)$ and the symmetrized Jacobian of a differentiable function ϕ by $\varepsilon[\phi] = (D\phi)^{\text{sym}}$. We denote by $\mathbb{1}$ both the identity map and the identity matrix. Finally, f_t refers to the evaluation of the function at time t , while \dot{f} refers to the temporal derivative of a differentiable function f .

Organization. This paper is organized as follows. In Section 2 we review the most important properties of the flow of diffeomorphism model and the metamorphosis model as its extension. In Section 3 the time continuous spline energy is derived and the proper interplay between Lagrangian and Eulerian perspective is discussed. Then, in Section 4 a variational time discretization of the continuous spline energy is introduced and the existence of discrete splines is studied. Section 5 represents the time extension of the time discrete quantities, which allows study of convergence to the time continuous model, presented in Section 6. Section 7 explains the fully discrete scheme and Section 8 shows how to set up a suitable iPALM algorithm to numerically solve for a spline interpolation given a set of key frames. Finally, Section 9 experimentally demonstrates properties of the spline approach for image metamorphosis and shows applications of the proposed method.

In comparison to the conference proceeding [JRR21] we present a significantly more detailed study of both time discrete and time continuous metamorphosis splines. We prove existence of discrete metamorphosis splines, give a suitable continuous extension of discrete metamorphosis splines and show that the discrete spline functional Γ -converges in the sense of Mosco to the continuous spline functional. This in particular enables to establish the existence of continuous metamorphosis splines as minimizers of the continuous spline energy. Furthermore, we extended the application section.

2 Review of Metamorphosis model

In this section, we briefly review the classical flow of diffeomorphism model and the metamorphosis model as its generalization.

2.1 Flow of diffeomorphism

In the flow of diffeomorphism model, the temporal change of c -channel image intensities $(u_t)_{t \in [0,1]} : \Omega \rightarrow \mathbb{R}^c$, is determined by a family of diffeomorphisms $(\psi_t)_{t \in [0,1]} : \bar{\Omega} \rightarrow \mathbb{R}^d$ describing a flow transporting image intensities along particle paths. This transport is given in terms of the equation $u_t(\cdot) = u_0 \circ \psi_t^{-1}(\cdot)$ also known as *brightness constancy assumption*, which is equivalent to a vanishing material derivative $\frac{D}{Dt}u = \dot{u} + v \cdot Du$, where $v_t = \dot{\psi}_t \circ \psi_t^{-1}$ denotes the time-dependent Eulerian velocity. The Riemannian space of images is endowed with the path energy

$$\mathcal{E}_{\psi_t}[(\psi_t)_{t \in [0,1]}] = \int_0^1 g_{\psi_t}(\dot{\psi}_t, \dot{\psi}_t) dt,$$

where the metric is given by

$$g_{\psi_t}(\dot{\psi}_t, \dot{\psi}_t) = \int_{\Omega} L[v, v] \, dx.$$

Here, L defines a quadratic form corresponding to a higher order elliptic operator. The specific choice, used throughout this paper is

$$L[v, v] = \text{tr}(\varepsilon[v]^2) + \gamma |D^m v|^2, \quad m > 1 + \frac{d}{2}, \gamma > 0. \quad (1)$$

In this case the metric $g_{\psi_t}(\dot{\psi}_t, \dot{\psi}_t)$ describes the viscous dissipation in a multipolar fluid model as investigated by Nečas and Šilhavý [NŠ91]. The first term of the integrand represents the dissipation density in a simple Newtonian fluid and the second term can be regarded as a higher order measure of the fluid friction. Given two image intensity functions u_A, u_B , an associated geodesic path is a family of images subject to the constraint $u_0 = u_A$, $u_1 = u_B$ and $u_t(\cdot) = u_A \circ \psi_t^{-1}(\cdot)$ where the family of diffeomorphisms minimizes the path energy.

We refer the reader to [DGM98, BMTY05, JM00, MTY02] for further details.

2.2 Metamorphosis model

The metamorphosis approach originally proposed by Miller, Trounev, Younes and coworkers in [MY01, TY05b, TY05a] generalizes the flow of diffeomorphism model by allowing for image intensity variations along motion paths and penalizing the squared material derivative in the metric. Under the assumption that the image path u is sufficiently smooth, the metric and the path energy read as

$$\begin{aligned} g(\dot{u}, \dot{u}) &= \min_{v: \Omega \rightarrow \mathbb{R}^d} \int_{\Omega} L[v, v] + \frac{1}{\delta} \left| \frac{D}{\partial t} u \right|^2 \, dx, \\ \mathcal{E}[u] &= \int_0^1 g(\dot{u}_t, \dot{u}_t) \, dt. \end{aligned} \quad (2)$$

Hence, the flow of diffeomorphism model is the limit case of the metamorphosis model for $\delta \rightarrow 0$.

Since paths in the space of images do not exhibit any time nor space smoothness properties in general, the evaluation of the material derivative is not well-defined. As a solution to these problems, Trounev and Younes [TY05a] proposed a nonlinear geometric structure in the space of images $\mathcal{I} := L^2(\Omega, \mathbb{R}^c)$. In detail, for a given image path $u \in L^2([0, 1], \mathcal{I})$ and an associated velocity field $v \in L^2((0, 1), \mathcal{V})$, where $\mathcal{V} := H^m(\Omega, \mathbb{R}^d) \cap H_0^1(\Omega, \mathbb{R}^d)$, we define the vector valued *weak material derivative* $\hat{z} \in L^2((0, 1), L^2(\Omega, \mathbb{R}^c))$ by

$$\int_0^1 \int_{\Omega} \eta \hat{z} \, dx \, dt = - \int_0^1 \int_{\Omega} (\partial_t \eta + \text{div}(v\eta)) u \, dx \, dt,$$

for a smooth test function $\eta \in C_c^\infty((0, 1) \times \Omega)$. With further consideration of equivalence classes of motion fields and material derivatives inducing the same temporal change of the image intensity we can consider (v, \hat{z}) as a tangent vector in the tangent space of \mathcal{I} at the image u and write $(v, \hat{z}) \in T_u \mathcal{I}$. This gives rise to the notion $H^1([0, 1], \mathcal{I})$ for regular paths in the space of images. The *path energy in the metamorphosis model* for a regular path $u \in H^1([0, 1], \mathcal{I})$ is then defined as

$$\mathcal{E}[u] = \int_0^1 \inf_{(v, \hat{z}) \in T_u \mathcal{I}} \int_{\Omega} L[v, v] + \frac{1}{\delta} |\hat{z}|^2 \, dx \, dt. \quad (3)$$

Image morphing of two input images $u_A, u_B \in \mathcal{I}$ then amounts to computing a shortest geodesic path $u \in H^1([0, 1], \mathcal{I})$ in the metamorphosis model, which is defined as a minimizer of the path energy in the class of regular curves such that $u(0) = u_A$ and $u(1) = u_B$. The infimum in (3) is attained, which is shown in [TY05a, Proposition 1 & Theorem 2] and the existence of a shortest geodesic is proven in [TY05a, Theorem 6].

The Lagrangian formulation of variation of the image intensity along motion trajectories is

$$u_t \circ \psi_t - u_s \circ \psi_s = \int_s^t \hat{z}_r \circ \psi_r \, dr, \quad \forall s, t \in [0, 1]. \quad (4)$$

This motivates a relaxed approach proposed in [ENR20, EKP⁺21], where the material derivative quantity is retrieved from a variational inequality

$$|u(t, \psi_t(x)) - u(s, \psi_s(x))| \leq \int_s^t z(r, \psi_r(x)) \, dr \quad (5)$$

for a.e. $x \in \Omega$ and all $1 \geq t > s \geq 0$. Formally, the scalar valued $z = |\hat{z}|$ replaces the actually vector-valued material derivative. In fact, given a path u in $L^2([0, 1], \mathcal{I})$ the inequality (5) defines a set $\mathcal{C}(u) \subset L^2((0, 1), \mathcal{V}) \times L^2((0, 1) \times \Omega)$ of admissible pairs $(v, z) \in \mathcal{C}(u)$ of the velocity and scalar weak material derivative fulfilling this inequality. Then the geodesic energy for a path $u \in L^2([0, 1], \mathcal{I})$ is defined by

$$\mathcal{E}[u] = \int_0^1 \inf_{(v, z) \in \mathcal{C}(u)} \int_{\Omega} L[v, v] + \frac{1}{\delta} z^2 \, dx \, dt. \quad (6)$$

The equivalence of the approaches (3) and (6) follows from [ENR20, Proposition 8], in the sense that for every z satisfying (5) there exists a \hat{z} satisfying (4) with $|\hat{z}| \leq z$ and for every \hat{z} satisfying (4) we have that $z = |\hat{z}|$ satisfies (5). Furthermore, for every $u \in L^2([0, 1], \mathcal{I})$ with non-empty $\mathcal{C}[u]$ one can show that $u \in C^0([0, 1], \mathcal{I})$ (cf. [EKP⁺21, Remark 1]), which allows point evaluation in time. In both [ENR20, EKP⁺21] the existence of continuous time geodesic paths was shown, where the relaxed approach turned out to be very natural.

3 Time continuous splines in metamorphosis model

In this section we introduce the time continuous splines in metamorphosis model. We ask for spline interpolation $(u_t)_{t \in [0, 1]}$ given a set of J key frames $u_j^I \in \mathcal{I}$ with constraints

$$u_{t_j} = u_j^I, \quad t_j \in [0, 1], \quad j = 1, \dots, J. \quad (7)$$

To this end, we recall that cubic splines in Euclidean space minimize the integral over the squared motion acceleration subject to position constraints [dB63], whereas linear interpolation is associated with the minimization of the integral over the squared motion velocity. In our case, image morphing via minimization of the path energy (2) corresponds to this linear interpolation. Here, we introduce the acceleration quantities which will be penalized in the spline energy. The Eulerian flow acceleration is defined by

$$a_t \circ \psi_t = \ddot{\psi}_t = \frac{d}{dt}(v_t \circ \psi_t) = \dot{v}_t \circ \psi_t + Dv_t \circ \psi_t \cdot v_t \circ \psi_t, \quad (8)$$

and for image paths with enough smoothness the second order material derivative is given by

$$\frac{D^2}{dt^2} u = \frac{d}{dt}(u_t + v_t \cdot Du_t) = \ddot{u}_t + v_t \cdot D\dot{u}_t + Du_t \cdot (\dot{v}_t + Dv_t v_t) + v_t \cdot (D\dot{u}_t + D^2 u_t v_t). \quad (9)$$

This splitting of acceleration term into flow acceleration and second order change of image intensity does not fully correspond to a Riemannian manifold approach since the stronger interference of the two entities is observed in the covariant derivative of the vector field $(v, \frac{D}{dt}u)$. Our model comes with the advantage that the splitting of the acceleration terms in physical more intuitive. The derivation of a spline model requires to minimize integrals over quadratic acceleration quantities, one is naturally led to the following still formal spline energy:

$$\mathcal{F}[u] := \min_v \int_0^1 \int_{\Omega} L[a, a] + \frac{1}{\delta} \left| \frac{D^2}{dt^2} u \right|^2 dx dt,$$

where for the simplicity we use the same elliptic operator (1).

As in the case of geodesic path energy, we give rigorous formulations for general paths $u \in L^2((0, 1), \mathcal{I})$. We observe the pairs $(v, a) \in L^2((0, 1), \mathcal{V}) \times L^2((0, 1), \mathcal{V})$ which determine the system

$$\begin{aligned} v_t(\psi_t(x)) &= \dot{\psi}_t(x), \quad \psi_0(x) = x \\ a_t(\psi_t(x)) &= \ddot{\psi}_t(x). \end{aligned}$$

Notice that from (8), one expects that the acceleration has one derivative less in comparison to the velocity. However, the approach we later take allows us to have the same number of derivatives. A similar gain of smoothness was noticed in [Via20].

Similar to (4) the Lagrangian formulation of the material acceleration $\hat{w} \in L^2((0, 1), L^2(\Omega, \mathbb{R}^c))$ is given by

$$\int_s^t \hat{w}_r \circ \psi_r dr = \hat{z}_t \circ \psi_t - \hat{z}_s \circ \psi_s.$$

By further using (4) we have

$$\begin{aligned} & \int_0^\tau \int_s^t \hat{w}_{r+l} \circ \psi_{r+l} dr dl \\ &= \int_0^\tau \hat{z}_{t+\tau} \circ \psi_{t+\tau} - \hat{z}_{s+\tau} \circ \psi_{t+\tau} dl \\ &= (u_{t+\tau} \circ \psi_{t+\tau} - u_t \circ \psi_t) - (u_{s+\tau} \circ \psi_{s+\tau} - u_s \circ \psi_s), \end{aligned} \tag{10}$$

for all $s, t \in (0, 1)$ and every τ , such that $t + \tau, s + \tau \in [0, 1]$. Observe that for $s = t - \tau$ the right hand side of (10) is an integral version of the second order central difference. Because there is no differentiation involved in these definitions, they work for general image paths. Analogous to (5), we introduce the scalar quantity $w \in L^2((0, 1) \times \Omega)$ as an relaxation of the weak second order material derivative

$$\int_0^\tau \int_s^t w_{r+l} \circ \psi_{r+l} dr dl \geq |u_{t+\tau} \circ \psi_{t+\tau} - u_t \circ \psi_t - u_{s+\tau} \circ \psi_{s+\tau} + u_s \circ \psi_s|. \tag{11}$$

This relaxed Lagrangian approach is substantially more handsome in comparison to the Eulerian approach (9) which will be exploited in the proof of consistency of continuous and time discrete approaches.

We can show the equivalence of the two approaches corresponding to (10) and (11).

Proposition 1. *For every vector valued (\hat{z}, \hat{w}) satisfying (4) and (10) there exist scalar quantities (z, w) satisfying (5) and (11) with $z = |\hat{z}|$ and $w = |\hat{w}|$. Conversely, for every (z, w) satisfying (5) and (11) there exists (\hat{z}, \hat{w}) satisfying (4) and (10) with $z \geq |\hat{z}|$ and $w \geq |\hat{w}|$.*

Proof. The first claim is obvious by the triangle inequality. To prove the converse, let z satisfy (5). We have

$$\|u_t \circ \psi_t - u_s \circ \psi_s\|_{L^2(\Omega)} \leq \int_s^t \|z_r \circ \psi_r\|_{L^2(\Omega)} dr,$$

from where we conclude that the function $t \mapsto u_t \circ \psi_t$ is in $AC^2([0, 1], L^2(\Omega))$ implying the a.e. differentiability and the existence of derivative $z' \in L^2((0, 1), L^2(\Omega, \mathbb{R}^c))$ such that

$$u_t \circ \psi_t - u_s \circ \psi_s = \int_s^t z'_r dr = \int_s^t \hat{z}_r \circ \psi_r dr$$

where $\hat{z}_r := z'_r \circ \psi_r^{-1}$ and $|\hat{z}| \leq z$. Thus, we have verified (4). This implies

$$\left| \int_0^\tau \hat{z}_{t+l} \circ \psi_{t+l} - \hat{z}_{s+l} \circ \psi_{s+l} dl \right| \leq \int_0^\tau \int_s^t w_{r+l} \circ \psi_{r+l} dr dl$$

and the analogous estimate for differentiation on interval $[-\tau, 0]$ for $\tau > 0$. Taking the limit as τ tends to zero we conclude that for a.e. $s \leq t \in [0, 1]$ and a.e. $x \in \Omega$ we have

$$\left| \hat{z}_t \circ \psi_t - \hat{z}_s \circ \psi_s \right| \leq \int_s^t w_r \circ \psi_r dr.$$

Thus, we can repeat the above procedure to conclude the existence of $\hat{w} \in L^2((0, 1), L^2(\Omega, \mathbb{R}^c))$ satisfying

$$\hat{z}_t \circ \psi_t - \hat{z}_s \circ \psi_s = \int_s^t \hat{w}_r \circ \psi_r dr, \quad |\hat{w}| \leq w,$$

from where the claim directly follows. \square

In [HRW18] a regularization of the spline path energy by addition of weighted geodesic path energy was necessary for existence and further analysis of the splines. We follow the analogous approach which seems to be unavoidable also in our model.

Definition 1 (Regularized spline energy). *Let $\sigma > 0$, $m > 1 + \frac{d}{2}$ be integers and $u \in L^2((0, 1), \mathcal{I})$ be an image curve. Then the regularized spline energy is defined by*

$$\mathcal{F}^\sigma[u] := \inf_{(v, a, z, w) \in \mathcal{C}[u]} \int_0^1 \int_\Omega L[a, a] + \frac{1}{\delta} w^2 + \sigma \left(L[v, v] + \frac{1}{\delta} z^2 \right) dx dt, \quad (12)$$

where $\mathcal{C}[u] \subset L^2((0, 1), \mathcal{V}) \times L^2((0, 1), \mathcal{V}) \times L^2((0, 1) \times \Omega) \times L^2((0, 1) \times \Omega)$ consists of tuples (v, a, z, w) satisfying

$$v_t(\psi_t(t, x)) = \dot{\psi}_t(x), \quad \psi_0(x) = x, \quad (13)$$

$$a_t(\psi_t(x)) = \ddot{\psi}_t(x), \quad (14)$$

$$|u_t \circ \psi_t - u_s \circ \psi_s| \leq \int_s^t z_r \circ \psi_r dr, \quad (15)$$

$$|u_{t+\tau} \circ \psi_{t+\tau} - u_t \circ \psi_t - u_{s+\tau} \circ \psi_{s+\tau} + u_s \circ \psi_s| \leq \int_0^\tau \int_s^t w_{r+l} \circ \psi_{r+l} dr dl. \quad (16)$$

The point evaluation of image path u is again possible if the set $\mathcal{C}[u]$ is non-empty. Motivated by [dB63], we now define the continuous time spline interpolation for given key frames.

Definition 2 (Continuous time regularized spline interpolation). *Let $\{u_j^I\}_{j=1,\dots,J} \in \mathcal{I}^J$. We call a minimizer $u \in L^2((0,1), \mathcal{I})$ of \mathcal{F}^σ that satisfies (7) a continuous time regularized spline interpolation of $\{u_j^I\}_{j=1,\dots,J}$ with regularity parameter σ .*

If we do not impose any additional constraints, we say the continuous time spline interpolation has natural boundary constraints. Imposing periodic boundary conditions are equivalent to defining the image curve u_t on the sphere \mathbb{S}^1 instead of the interval $[0,1]$. In case of Hermite boundary conditions, we ask for $v_0 = v_A, v_1 = v_B$ and, in light of Proposition 1 and differentiation of the left hand side of (4), that $\hat{z}_0 = \hat{z}_A$ and $\hat{z}_1 = \hat{z}_B$. Note that in the case of Hermite boundary conditions (also called clamped boundary conditions), we implicitly require $t_1 = 0$ and $t_J = 1$, so that u_0 and u_1 are also prescribed.

4 Variational time discretization

In this section we study the variational time discretization of the time continuous (regularized) spline energy. To this end, we pick up the approach of [BER15, EKP⁺21] for the variational time discretization of geodesic energy. We consider a discrete image curve $\mathbf{u} = (u_0, \dots, u_K)$ with $u_k \in \mathcal{I}$ and define a set of admissible deformations

$$\mathcal{D} := \{\phi \in H^m(\Omega, \Omega), \det(D\phi) \geq \epsilon, \phi = \mathbb{1} \text{ on } \partial\Omega\}, \quad (17)$$

for a fixed (small) $\epsilon > 0$, which consists of $C^1(\Omega, \Omega)$ -diffeomorphisms [Cia88, Theorem 5.5-2].

Remark 1. *The case $\epsilon = 0$ is discussed in Remark 3.*

Consider $\mathbf{u} \in \mathcal{I}^{K+1}$ as time sampling at points $\frac{k}{K}$, $k = 0, \dots, K$, of a smooth curve and $\Phi = (\phi_1, \dots, \phi_K) \in \mathcal{D}^K$ as relative flow ($\phi_k = \psi_{\frac{k}{K}} \circ \psi_{\frac{k-1}{K}}^{-1}$) and using backward finite difference approximations we obtain the discrete version of the Eulerian velocity $v_k := K(\phi_k - \mathbb{1})$ and $\hat{z}_k := K(u_k \circ \phi_k - u_{k-1})$ for the discrete material derivative. Furthermore, by using central finite difference we define the discrete acceleration

$$a_k := K^2((\phi_{k+1} - \mathbb{1}) \circ \phi_k - (\phi_k - \mathbb{1})) \quad (18)$$

and

$$\begin{aligned} \hat{w}_k &:= K(\hat{z}_k \circ \phi_k - \hat{z}_{k-1}) \\ &= K^2(u_{k+1} \circ \phi_{k+1} \circ \phi_k - 2u_k \circ \phi_k + u_{k-1}) \end{aligned} \quad (19)$$

as the discrete version of the second material derivative. Following [BER15, EKP⁺21] we consider the discrete path energy

$$\mathbf{E}^{K,D}[\mathbf{u}, \Phi] := K \sum_{k=1}^K \int_{\Omega} W_D(D\phi_k) + \gamma |D^m \phi_k|^2 + \frac{1}{\delta} |u_k \circ \phi_k - u_{k-1}|^2 \, dx,$$

where $W_D(B) := |B^{sym} - \mathbb{1}|^2$ is a simple elastic energy density. Then, the discrete counterpart of the spline energy is defined as

$$\mathbf{F}^{K,D}[\mathbf{u}, \Phi] := \frac{1}{K} \sum_{k=1}^{K-1} \int_{\Omega} W_A(Da_k) + \gamma |D^m a_k|^2 + \frac{1}{\delta} |\hat{w}_k|^2 \, dx, \quad (20)$$

with the energy density $W_A(B) := |B^{sym}|^2$. We note that $a_k \in H^m(\Omega, \mathbb{R}^d)$ by [IKT13]. Finally, the regularized discrete spline energy is given by

$$\mathbf{F}^{\sigma, K, D}[\mathbf{u}, \Phi] := \mathbf{F}^{K, D}[\mathbf{u}, \Phi] + \sigma \mathbf{E}^{K, D}[\mathbf{u}, \Phi].$$

As in the continuous time model we have interpolation constraints. Let $J^K = (i_1, \dots, i_{J^K})$ be an index tuple $2 \leq |J^K| \leq K$, $J^K \subset \{0, \dots, K\}$. We consider a $|J^K|$ -tuple $\mathcal{I}_f^K = (u_1^I, \dots, u_{J^K}^I)$ and define the set of admissible image vectors

$$\mathcal{I}_{adm}^K = \{\mathbf{u} \in \mathcal{I}^{K+1}, u_{i_j} = u_j^I, j = 1, \dots, J^K\}. \quad (21)$$

We are now in a position to define discrete splines.

Definition 3. Let $\mathbf{u} = (u_0, \dots, u_K) \in \mathcal{I}_{adm}^K$. Then we set

$$\mathbf{F}^{\sigma, K}[\mathbf{u}] := \inf_{\Phi \in \mathcal{D}^K} \mathbf{F}^{\sigma, K, D}[\mathbf{u}, \Phi]. \quad (22)$$

A discrete spline is a discrete $(K+1)$ -tuple that minimizes $\mathbf{F}^{\sigma, K}$ over all discrete paths in \mathcal{I}_{adm}^K .

The presented discretization is valid in the case of natural boundary conditions, to which we restrict in further discussions. We remark that in the case of periodic boundary conditions we make an identification $K \triangleq 0, K+1 \triangleq 1$ and the sum in (20) goes up to K . For the discrete version of Hermite boundary conditions we prescribe $\phi_1 = \bar{\phi}_1, \phi_K = \bar{\phi}_K, u_0 = \bar{u}_0, u_K = \bar{u}_K$ and $\hat{z}_1 = \bar{\hat{z}}_1, \hat{z}_K = \bar{\hat{z}}_K$ for given $\bar{\phi}_1, \bar{\phi}_K \in \mathcal{D}$, $\bar{u}_0, \bar{u}_K \in \mathcal{I}$ and $\bar{\hat{z}}_1, \bar{\hat{z}}_K \in L^2(\Omega, \mathbb{R}^c)$. Next, we follow ideas from [EKP⁺21] in order to prove the existence of discrete spline interpolations. The following lemma is the analogous result to [EKP⁺21, Lemma 1] and we only state it for completeness.

Lemma 1. There exists a constant C which only depends on Ω, m, d, γ such that

$$\|\phi - \mathbf{1}\|_{H^m(\Omega)} \leq C \sqrt{C_\phi}$$

for all $\phi \in \mathcal{D}$ satisfying $\int_\Omega W_D(D\phi) + \gamma |D^m \phi|^2 dx \leq C_\phi$.

Proof. An application of the Gagliardo–Nirenberg inequality [Nir66] yields

$$\|\phi - \mathbf{1}\|_{H^m(\Omega)} \leq C(\|\phi - \mathbf{1}\|_{L^2(\Omega)} + |\phi - \mathbf{1}|_{H^m(\Omega)}). \quad (23)$$

The last term in (23) is bounded by

$$|\phi - \mathbf{1}|_{H^m(\Omega)} = |\phi|_{H^m(\Omega)} \leq \sqrt{\frac{C_\phi}{\gamma}}. \quad (24)$$

To estimate the lower order term on the right hand side we use Korn's and Poincaré's inequality and write

$$\|\phi - \mathbf{1}\|_{L^2(\Omega)} \leq C\|\varepsilon[\phi] - \mathbf{1}\|_{L^2(\Omega)} \leq C\sqrt{C_\phi}. \quad (25)$$

Thus, the lemma follows by combining (23), (24) and (25). \square

Remark 2. The analogous result holds for the boundedness of acceleration i.e.

$$\int_\Omega W_A(Da) + \gamma |D^m a|^2 dx \leq C_a \text{ implies } \|a\|_{H^m(\Omega)} \leq C\sqrt{C_a}.$$

Now, we show the well-posedness of (22).

Proposition 2. For every $K \in \mathbb{N}$ and every image vector $\mathbf{u} = (u_0, \dots, u_K) \in \mathcal{I}^{K+1}$ there exists a deformation vector $\Phi = (\phi_1, \dots, \phi_K) \in \mathcal{D}^K$ such that

$$\mathbf{F}^{\sigma, K, D}[\mathbf{u}, \Phi] = \inf_{\tilde{\Phi} \in \mathcal{D}^K} \mathbf{F}^{\sigma, K, D}[\mathbf{u}, \tilde{\Phi}].$$

Proof. Let $\{\Phi^j\}_{j \in \mathbb{N}} \in \mathcal{D}^K$ be a sequence for which it holds $\lim_{j \rightarrow \infty} \mathbf{F}^{\sigma, K, D}[\mathbf{u}, \Phi^j] = \inf_{\tilde{\Phi} \in \mathcal{D}^K} \mathbf{F}^{\sigma, K, D}[\mathbf{u}, \tilde{\Phi}]$ and $\mathbf{F}^{\sigma, K, D}[\mathbf{u}, \Phi^j] \leq \overline{\mathbf{F}^{\sigma, K}} := \mathbf{F}^{\sigma, K, D}[\mathbf{u}, \mathbb{1}^K]$. By Lemma 1 we have

$$\|\phi_k^j - \mathbb{1}\|_{H^m(\Omega)} \leq C\sqrt{\overline{\mathbf{F}^{\sigma, K}}}, \quad \forall j \in \mathbb{N}, \quad k = 1, \dots, K.$$

Thus, $\{\Phi^j\}_{j \in \mathbb{N}}$ is uniformly bounded in $H^m(\Omega, \Omega)^K$. By reflexivity of this space there exists a subsequence (with the same label) such that $\Phi^j \rightharpoonup \Phi$ in $H^m(\Omega, \Omega)^K$. By the compact Sobolev embedding, we have $\Phi^j \rightarrow \Phi$ in $C^{1, \alpha}(\overline{\Omega}, \overline{\Omega})^K$, which gives us that $\Phi \in \mathcal{D}^K$. Analogously, we have boundedness of \mathbf{a}^j in $H^m(\Omega, \Omega)^{K-1}$ and thus a convergent subsequence satisfying $\mathbf{a}^j \rightharpoonup \mathbf{a}$ in $H^m(\Omega, \Omega)^{K-1}$ and $\mathbf{a}^j \rightarrow \mathbf{a}$ in $C^{1, \alpha}(\overline{\Omega}, \overline{\Omega})^{K-1}$. Here, for every $j \in \mathbb{N}$ we have $\mathbf{a}^j = (a_1^j, \dots, a_{K-1}^j)$ given by (18). From the strong convergence of deformations we have that $a_k = K^2(\phi_{k+1} \circ \phi_k - 2\phi_k + \mathbb{1})$ for all $k = 1, \dots, K-1$. Using weak lower semicontinuity of H^m -seminorm and continuity of energy densities we have for all k , as $j \rightarrow \infty$:

$$\begin{aligned} \liminf |\phi_k^j|_{H^m} &\geq |\phi_k|_{H^m}, \quad \|W_D(D\phi_k^j)\|_{L^1(\Omega)} \rightarrow \|W_D(D\phi_k)\|_{L^1(\Omega)}, \\ \liminf |a_k^j|_{H^m} &\geq |a_k|_{H^m}, \quad \|W_A(Da_k^j)\|_{L^1(\Omega)} \rightarrow \|W_A(Da_k)\|_{L^1(\Omega)}. \end{aligned} \quad (26)$$

To handle to rest of the terms we show that for all $u \in \mathcal{I}$ we have $u \circ \phi^j \rightarrow u \circ \phi$ in \mathcal{I} for $\{\phi^j\}_{j \in \mathbb{N}} \in \mathcal{D}$ with $\phi^j \rightarrow \phi$ in $C^1(\overline{\Omega}, \overline{\Omega})$ as $j \rightarrow \infty$. To see this we approximate u by smooth functions $\tilde{u}^i \in C^\infty(\overline{\Omega}, \overline{\Omega})$ with $\|\tilde{u} - \tilde{u}^i\|_{\mathcal{I}} \rightarrow 0$. Then, using the transformation formula we obtain

$$\begin{aligned} &\|u \circ \phi^j - u \circ \phi\|_{\mathcal{I}} \\ &\leq \|u \circ \phi^j - \tilde{u}^i \circ \phi^j\|_{\mathcal{I}} + \|\tilde{u}^i \circ \phi - u \circ \phi\|_{\mathcal{I}} + \|\tilde{u}^i \circ \phi^j - \tilde{u}^i \circ \phi\|_{\mathcal{I}} \\ &\leq \|u - \tilde{u}^i\|_{\mathcal{I}} \left(\|\det(D\phi^j)\|_{L^\infty(\Omega)}^{-\frac{1}{2}} + \|\det(D\phi)\|_{L^\infty(\Omega)}^{-\frac{1}{2}} \right) + \|D\tilde{u}^i\|_{L^\infty(\Omega)} \|\phi^j - \phi\|_{L^2(\Omega)}. \end{aligned} \quad (27)$$

By first choosing i and then j we have that this expression converges to 0. Hence, for every $k = 1, \dots, K$ we have $\|u_k \circ \phi_k^j - u_{k-1}\|_{\mathcal{I}} \rightarrow \|u_k \circ \phi_k - u_{k-1}\|_{\mathcal{I}}$. Furthermore, via nested application of (27) $\|u_{k+1} \circ \phi_{k+1}^j \circ \phi_k^j - 2u_k \circ \phi_k^j + u_{k-1}\|_{\mathcal{I}} \rightarrow \|u_{k+1} \circ \phi_{k+1} \circ \phi_k - 2u_k \circ \phi_k + u_{k-1}\|_{\mathcal{I}}$ for $k = 1, \dots, K-1$, which together with (26) finishes the proof. \square

In the next step, under suitable conditions, we prove that there exists a minimizing vector in \mathcal{I}_{adm}^K (see (21)) for a fixed deformation vector $\Phi \in \mathcal{D}^K$.

Proposition 3. Let $K \geq 2$, \mathcal{I}_f^K and $\Phi \in \mathcal{D}^K$ be fixed. Assume that the deformations satisfy, for every $x \in \Omega$,

$$C_{\det} \geq \det(D\phi_k(x)) \geq c_{\det} > 0, \quad k = 1, \dots, K. \quad (28)$$

Then there exists a vector of images $\mathbf{u} \in \mathcal{I}_{adm}^K$ such that

$$\mathbf{F}^{\sigma, K, D}[\mathbf{u}, \Phi] = \inf \{ \mathbf{F}^{\sigma, K, D}[\tilde{\mathbf{u}}, \Phi] : \tilde{\mathbf{u}} \in \mathcal{I}_{adm}^K \}.$$

Proof. Let $(\mathbf{u}^j)_{j \in \mathbb{N}} \in \mathcal{I}_{adm}^K$ be an approximation sequence such that

$$\lim_{j \rightarrow \infty} \mathbf{F}^{\sigma, K, D}[\mathbf{u}^j, \Phi] = \inf_{\tilde{\mathbf{u}} \in \mathcal{I}_{adm}^K} \mathbf{F}^{\sigma, K, D}[\tilde{\mathbf{u}}, \Phi] \leq \overline{\mathbf{F}^{\sigma, K, D}}.$$

Here, $\overline{\mathbf{F}^{\sigma,K,D}} := \mathbf{F}^{\sigma,K,D}[\bar{\mathbf{u}}, \Phi]$ represents a finite upper bound for the energy with the vector of images $\bar{\mathbf{u}}$ satisfying $\bar{u}_k = u_1^I$ for $k \leq i_1$ and $\bar{u}_k = u_j^I$ for $i_1 + 1 \leq k \leq i_j$ with $j \geq 2$. Indeed, we have

$$\begin{aligned} \overline{\mathbf{F}^{\sigma,K,D}} &\leq \sum_{k=1}^{K-1} \frac{1}{K} (\|W_A(Da_k)\|_{L^1(\Omega)} + \gamma \|a_k\|_{H^m}^2) \\ &\quad + \sigma \sum_{k=1}^K K (\|W_D(D\phi_k)\|_{L^1(\Omega)} + \gamma \|\phi_k\|_{H^m}^2) + K^3 (1 + c_{\det}^{-1})^2 \sum_{j=1}^{J^K} \|u_j^I\|_{\mathcal{I}}^2, \end{aligned}$$

where we used the transformation formula and (28). By further use of (28) we have

$$\begin{aligned} \|u_k^j\|_{\mathcal{I}} &\leq \|u_{k+1}^j \circ \phi_{k+1} - u_k^j\|_{\mathcal{I}} + \|u_{k+1}^j \circ \phi_{k+1}\|_{\mathcal{I}} \leq \sqrt{\frac{\delta \mathbf{F}^{\sigma,K,D}}{K}} + c_{\det}^{-\frac{1}{2}} \|u_{k+1}^j\|_{\mathcal{I}}, \\ \|u_{k+1}^j\|_{\mathcal{I}} &\leq C_{\det}^{-\frac{1}{2}} \|u_{k+1}^j \circ \phi_{k+1}\|_{\mathcal{I}} \\ &\leq C_{\det}^{-\frac{1}{2}} (\|u_{k+1}^j \circ \phi_{k+1} - u_k^j\|_{\mathcal{I}} + \|u_k^j\|_{\mathcal{I}}) \leq C_{\det}^{-\frac{1}{2}} \left(\sqrt{\frac{\delta \mathbf{F}^{\sigma,K,D}}{K}} + \|u_k^j\|_{\mathcal{I}} \right), \end{aligned} \quad (29)$$

from where we have, by induction, that u_k^j is uniformly bounded in \mathcal{I} for every $k = 0, \dots, K$. By reflexivity, there exists a subsequence (labelled in the same way) such that $u_k^j \rightharpoonup u_k$ for some $\mathbf{u} \in \mathcal{I}_{adm}^K$. It remains to verify the weak lower semi-continuity of the matching functional, i.e. we have to show that

$$\|u_k \circ \phi_k - u_{k-1}\|_{\mathcal{I}}^2 \leq \liminf_{j \rightarrow \infty} \|u_k^j \circ \phi_k - u_{k-1}^j\|_{\mathcal{I}}^2, \quad (30)$$

$$\|u_{k+1} \circ \phi_{k+1} \circ \phi_k - 2u_k \circ \phi_k + u_{k-1}\|_{\mathcal{I}}^2 \leq \liminf_{j \rightarrow \infty} \|u_{k+1}^j \circ \phi_{k+1} \circ \phi_k - 2u_k^j \circ \phi_k + u_{k-1}^j\|_{\mathcal{I}}^2, \quad (31)$$

for every $k = 1, \dots, K$ and $k = 1, \dots, K-1$, respectively. To this end, we first show $u_k^j \circ \phi_k \rightharpoonup u_k \circ \phi_k$ in \mathcal{I} . For every $v \in \mathcal{I}$ the transformation formula yields

$$\int_{\Omega} (u_k^j \circ \phi_k - u_k \circ \phi_k) \cdot v \, dx = \int_{\Omega} (u_k^j - u_k) \cdot (v(\det(D\phi_k))^{-1}) \circ \phi_k^{-1} \, dx,$$

which converges to 0 since $(v(\det(D\phi_k))^{-1}) \circ \phi_k^{-1} \in \mathcal{I}$ due to (28). Hence, $u_k^j \circ \phi_k - u_{k-1}^j \rightharpoonup u_k \circ \phi_k - u_{k-1}$ in \mathcal{I} , which readily implies (30) and by applying the same technique in a nested fashion we get (31). Altogether, we have

$$\liminf_{j \rightarrow \infty} \mathbf{F}^{\sigma,K,D}[\mathbf{u}^j, \Phi] \geq \mathbf{F}^{\sigma,K,D}[\mathbf{u}, \Phi],$$

from where the optimality follows. \square

We are now in the position to show the existence of discrete splines.

Theorem 1. *Let $K \geq 2$. Then for every \mathcal{I}_f^K there exists $\mathbf{u} \in \mathcal{I}_{adm}^K$ such that*

$$\mathbf{F}^{\sigma,K}[\mathbf{u}] = \inf_{\mathbf{v} \in \mathcal{I}_{adm}^K} \mathbf{F}^{\sigma,K}[\mathbf{v}].$$

Proof. Consider a sequence $\mathbf{u}^j \in \mathcal{I}_{adm}^K$ for which it holds $\lim_{j \rightarrow \infty} \mathbf{F}^{\sigma,K}[\mathbf{u}^j] = \inf_{\mathbf{v} \in \mathcal{I}_{adm}^K} \mathbf{F}^{\sigma,K}[\mathbf{v}] \leq \overline{\mathbf{F}^{\sigma,K}}$, where $\overline{\mathbf{F}^{\sigma,K}} := \mathbf{F}^{\sigma,K,D}[\bar{\mathbf{u}}^I, \mathbf{1}^K]$ and $\bar{\mathbf{u}}^I$ is a vector of images made by linear interpolation between each two consecutive fixed images (see (21)). We have

$$\overline{\mathbf{F}^{\sigma,K}} \leq \left(\frac{\sigma}{\delta} + \frac{2K}{\delta(t_{j+1}^K - t_j^K)^2} \right) \sum_{j=1}^{J^K-1} \|u_{j+1}^I - u_j^I\|^2 < \infty,$$

where $t_j^K = \frac{t_j}{K}$. Furthermore, for every j let, by Proposition 2, $\mathbf{F}^{\sigma,K}[\mathbf{u}^j] = \mathbf{F}^{\sigma,K,D}[\mathbf{u}^j, \Phi^j]$. As in the proof of Proposition 2 we have weak convergence of Φ^j in $H^m(\Omega, \Omega)^K$ and strong in $C^{1,\alpha}(\overline{\Omega}, \overline{\Omega})^K$ to some $\Phi \in \mathcal{D}^K$. Furthermore, we again have $a_k^j \rightharpoonup a_k$ in $H^m(\Omega, \Omega)$, and strongly in $C^{1,\alpha}(\overline{\Omega}, \overline{\Omega})$, where $a_k = K^2(\phi_{k+1} \circ \phi_k - 2\phi_k + \mathbf{1})$ and estimates from (26) are satisfied. By Proposition 3 we may replace \mathbf{u}^j by an energy optimal image vector. Keeping the same label and following the same arguments as in (29) we conclude that \mathbf{u}^j is uniformly bounded in \mathcal{I} , weakly converging to \mathbf{u} . We are left to verify the estimates

$$\begin{aligned} \|u_k \circ \phi_k - u_{k-1}\|_{\mathcal{I}}^2 &\leq \liminf_{j \rightarrow \infty} \|u_k^j \circ \phi_k^j - u_{k-1}^j\|_{\mathcal{I}}^2, \\ \|u_{k+1} \circ \phi_{k+1} \circ \phi_k - 2u_k \circ \phi_k + u_{k-1}\|_{\mathcal{I}}^2 &\leq \liminf_{j \rightarrow \infty} \|u_{k+1}^j \circ \phi_{k+1}^j \circ \phi_k^j - 2u_k^j \circ \phi_k^j + u_{k-1}^j\|_{\mathcal{I}}^2, \end{aligned}$$

for every $k = 1, \dots, K$ and $k = 1, \dots, K-1$, respectively. To that end, it is enough to show $u_k^j \circ \phi_k^j \rightharpoonup u_k \circ \phi_k$ in \mathcal{I} . To see this, we first take into account the decomposition

$$u_k^j \circ \phi_k^j - u_k \circ \phi_k = (u_k^j \circ \phi_k^j - u_k \circ \phi_k^j) + (u_k \circ \phi_k^j - u_k \circ \phi_k). \quad (32)$$

The second term is handled as in (27). It remains to consider the convergence properties of the first term. For a test function $v \in \mathcal{I}$ we obtain using the transformation rule

$$\int_{\Omega} (u_k^j \circ \phi_k^j - u_k \circ \phi_k^j) \cdot v \, dx = \int_{\Omega} (u_k^j - u_k) \cdot (v(\det(D\phi_k^j))^{-1} \circ (\phi_k^j)^{-1}) \, dx.$$

The right hand side converges to 0 due to the convergence $(\det(D\phi_k^j))^{-1} \circ (\phi_k^j)^{-1} \rightarrow \det(D\phi_k)^{-1} \circ \phi_k^{-1}$ in $L^\infty(\Omega)$, $v \circ \phi_k^j \rightarrow v \circ \phi_k$ in \mathcal{I} and $u_k^j \rightharpoonup u_k$ in \mathcal{I} for $j \rightarrow \infty$. This proves our claim and finally proves the theorem. \square

Remark 3. *The results of this section remain valid for any W_D satisfying conditions (W1)–(W3) from [EKP⁺21]. Furthermore, for large enough K one can show the existence of the discrete spline even if $\epsilon = 0$ in the definition of the admissible set. Namely, as in Theorem 1 one can construct a finite upper bound $\overline{\mathbf{F}}^{\sigma,K}$ for the spline energy independent of K (see the proof of Theorem 3). Then, using Lemma 1, Sobolev embedding theorem and Lipschitz continuity of the determinant we have, for large enough K , $\max_{k=1,\dots,K} \|\det(D\phi_k) - 1\|_{L^\infty(\Omega)} \leq C\sqrt{\frac{\overline{\mathbf{F}}^{\sigma,K}}{K}} < 1$, which proves $\min_{k=1,\dots,K} \det(D\phi_k) \geq c_{\det} > 0$ and we can proceed as before.*

5 Temporal extension operators

In this section we define the suitable time extensions of the time discrete quantities from the previous section. This is necessary to compare discrete and continuous spline functional and to study convergence.

Let $K \geq 2$, $\tau = \frac{1}{K}$, $t_k^K = k\tau$, $t_{k \pm \frac{1}{2}}^K = (k \pm \frac{1}{2})\tau$, $k = 0, 1, \dots, K$. Furthermore, consider a vector of images $\mathbf{u}^K = (u_0^K, \dots, u_K^K) \in \mathcal{I}^{K+1}$ and a vector of deformations $\Phi^K = (\phi_1^K, \dots, \phi_K^K) \in \mathcal{D}^K$. We first define a *discrete incremental transport path* y^K with $y_t^K = y_0^K(t, \cdot)$ for $t \in [0, t_{\frac{1}{2}}^K]$, $y_t^K = y_k^K(t, \cdot)$ for $t \in [t_{k-\frac{1}{2}}^K, t_{k+\frac{1}{2}}^K]$ with $k = 1, \dots, K-1$ and $y_t^K = y_K^K(t, \cdot)$ for $t \in [t_{K-\frac{1}{2}}^K, 1]$, where

$$\begin{aligned} y_0^K(t, \cdot) &= \mathbf{1} + \frac{t}{\tau}(\phi_1^K - \mathbf{1}) \\ y_k^K(t, \cdot) &= \mathbf{1} + \frac{t - t_{k-\frac{1}{2}}^K}{\tau}(\phi_k^K - \mathbf{1}) \end{aligned}$$

and, for $k = 1, \dots, K-1$

$$y_k^K(t, \cdot) = \frac{1}{2}(\mathbb{1} + \phi_k^K) + \frac{t-t_{k-\frac{1}{2}}^K}{\tau}(\phi_k^K - \mathbb{1}) + \frac{(t-t_{k-\frac{1}{2}}^K)^2}{2\tau^2}(\phi_{k+1}^K \circ \phi_k^K - 2\phi_k^K + \mathbb{1}).$$

This can be seen as the cubic Hermite interpolation on intervals $[t_{k-\frac{1}{2}}^K, t_{k+\frac{1}{2}}^K]$, and an affine interpolation on $[0, t_{\frac{1}{2}}^K)$ and $(t_{K-\frac{1}{2}}^K, 1]$. In particular, observe that $y_{t_{k-\frac{1}{2}}^K}^K = \frac{\mathbb{1} + \phi_k^K}{2}$ and $y_{t_{k+\frac{1}{2}}^K}^K = \frac{(\mathbb{1} + \phi_{k+1}^K) \circ \phi_k^K}{2}$ with the corresponding slopes $\frac{\phi_k^K - \mathbb{1}}{\tau}$ and $\frac{(\phi_{k+1}^K - \mathbb{1}) \circ \phi_k^K}{\tau}$, respectively. We define the *image extension operator* $\mathcal{U}^K[\mathbf{u}^K, \Phi^K] \in L^2([0, 1], \mathcal{I})$ as $\mathcal{U}^K[\mathbf{u}^K, \Phi^K](t, x) = u^K(t, x)$ where

$$\begin{aligned} u_t^K \circ y_t^K &= u_0^K + \frac{t}{\tau}(u_1^K \circ \phi_1^K - u_0^K), \quad t \in [0, t_{\frac{1}{2}}^K) \\ u_t^K \circ y_t^K &= u_{K-1}^K + \frac{t-t_{K-\frac{1}{2}}^K}{\tau}(u_K^K \circ \phi_K^K - u_{K-1}^K), \quad t \in [t_{K-\frac{1}{2}}^K, 1] \end{aligned}$$

and, for $k = 1, \dots, K-1$ and $t \in [t_{k-\frac{1}{2}}^K, t_{k+\frac{1}{2}}^K)$

$$\begin{aligned} &u_t^K \circ y_t^K \\ &= \frac{u_{k-1}^K + u_k^K \circ \phi_k^K}{2} + \frac{t-t_{k-\frac{1}{2}}^K}{\tau}(u_k^K \circ \phi_k^K - u_{k-1}^K) + \frac{(t-t_{k-\frac{1}{2}}^K)^2}{2\tau^2}(u_{k+1}^K \circ \phi_{k+1}^K \circ \phi_k^K - 2u_k^K \circ \phi_k^K + u_{k-1}^K). \end{aligned} \quad (33)$$

This can be seen as blending between the "half-way images" $\frac{u_{k-1}^K + u_k^K \circ \phi_k^K}{2}$ and $\frac{(u_k^K + u_{k+1}^K \circ \phi_{k+1}^K) \circ \phi_k^K}{2}$ along the incremental transport path y^K . This is depicted on Fig. 1.

The discrete velocity field corresponding to the discrete incremental transport path y_t^K is given by

$$v_0^K(t, \cdot) = \frac{1}{\tau}(\phi_1^K - \mathbb{1}), \quad v_K^K(t, \cdot) = \frac{1}{\tau}(\phi_K^K - \mathbb{1}),$$

for $t \in [0, t_{\frac{1}{2}}^K)$ and $t \in [t_{K-\frac{1}{2}}^K, 1]$, respectively, and

$$v_k^K(t, \cdot) = \frac{1}{\tau}(\phi_k^K - \mathbb{1}) + \frac{t-t_{k-\frac{1}{2}}^K}{\tau^2}(\phi_{k+1}^K \circ \phi_k^K - 2\phi_k^K + \mathbb{1}),$$

for $t \in [t_{k-\frac{1}{2}}^K, t_{k+\frac{1}{2}}^K)$ with $k = 1, \dots, K-1$. The corresponding discrete acceleration is $a_0^K(t, \cdot) = a_K^K(t, \cdot) = 0$ for $t \in [0, t_{\frac{1}{2}}^K)$ and $t \in [t_{K-\frac{1}{2}}^K, 1]$, respectively, and

$$a_k^K(t, \cdot) = \frac{1}{\tau^2}(\phi_{k+1}^K \circ \phi_k^K - 2\phi_k^K + \mathbb{1}),$$

for $t \in [t_{k-\frac{1}{2}}^K, t_{k+\frac{1}{2}}^K)$ with $k = 1, \dots, K-1$. The spatial inverse of the discrete incremental transport path is denoted by $x_k^K(t, \cdot)$, $k = 0, \dots, K$ which, following [Cia88, Chapter 5] exists if $\max_{k=1, \dots, K} \|D\phi_k^K - \mathbb{1}\|_{C^0(\Omega)} < c$ for a small enough constant $c > 0$ (see Section 6). We define the velocity and the acceleration along the incremental transport path by

$$\tilde{v}_t^K = v_t^K \circ x_t^K, \quad \tilde{a}_t^K = a_t^K \circ x_t^K. \quad (34)$$

Now, the actual discrete flow given as the map $(t, x) \mapsto \psi_t^K(x)$ is defined recursively by

$$\begin{aligned} \psi_t^K &:= y_0^K(t, \cdot), \quad t \in [0, t_{\frac{1}{2}}^K), \\ \psi_t^K &:= y_k^K(t, \psi_{t_{k-\frac{1}{2}}^K}^K(\cdot)), \quad t \in [t_{k-\frac{1}{2}}^K, t_{k+\frac{1}{2}}^K]. \end{aligned} \quad (35)$$

One can directly show that (35) is well-defined in the sense of equations (13) – (14), i.e.

$$\begin{aligned}\dot{\psi}_t^K &= \dot{v}_t^K \circ \psi_t^K, \quad \psi_0^K(x) = x \\ \ddot{\psi}_t^K &= \ddot{a}_t^K \circ \psi_t^K.\end{aligned}$$

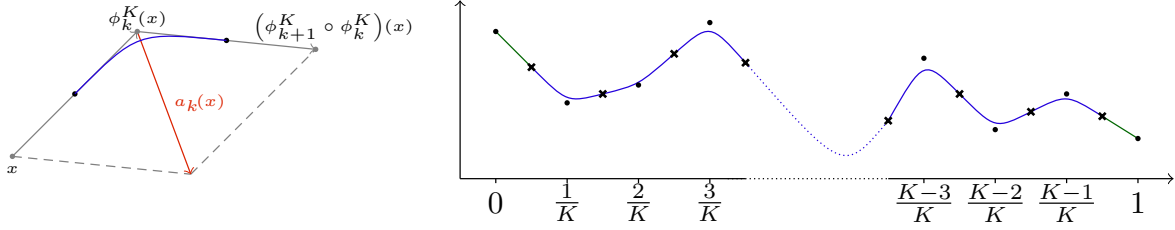


Figure 1: Left: Schematic drawing of the Hermite interpolation (blue) on the time interval $[(k - \frac{1}{2})/K, (k + \frac{1}{2})/K]$ together with the discrete acceleration $a_k^K(x)$. Right: Image extension $\mathcal{U}^K[\mathbf{u}^K, \Phi^K](\cdot, x)$ along a path $(\psi_t^K(x))_{t \in [0,1]}$ from the left, plotted against time. Dots represent the values u_k^K , and crosses the "half-way" values $\frac{1}{2}(u_k^K + u_{k-1}^K)$ along the discrete transport path.

Based on this, the first order scalar weak material derivative of u^K can be defined as the absolute value of the material derivative along the paths $t \mapsto \psi_t^K(x)$ with

$$\begin{aligned}z_t^K \circ y_t^K &= \frac{1}{\tau} |u_1^K \circ \phi_1^K - u_0^K|, \quad t \in [0, t_{\frac{1}{2}}^K) \\ z_t^K \circ y_t^K &= \frac{1}{\tau} |u_K^K \circ \phi_K^K - u_{K-1}^K|, \quad t \in [t_{K-\frac{1}{2}}^K, 1],\end{aligned}$$

and

$$z_t^K \circ y_t^K = \left| \frac{1}{\tau} (u_k^K \circ \phi_k^K - u_{k-1}^K) \frac{t - t_{k-\frac{1}{2}}^K}{\tau^2} (u_{k+1}^K \circ \phi_{k+1}^K \circ \phi_k^K - 2u_k^K \circ \phi_k^K + u_{k-1}^K) \right|,$$

for $t \in [t_{k-\frac{1}{2}}^K, t_{k+\frac{1}{2}}^K)$, $k = 1, \dots, K-1$. For the second order scalar weak material derivative we have that for $t \in [t_{k-\frac{1}{2}}^K, t_{k+\frac{1}{2}}^K)$, $k = 1, \dots, K-1$

$$w_t^K \circ y_t^K = \frac{1}{\tau^2} |u_{k+1}^K \circ \phi_{k+1}^K \circ \phi_k^K - 2u_k^K \circ \phi_k^K + u_{k-1}^K|,$$

and $w_t^K = 0$ elsewhere, which is the absolute value of the second time derivative of $\mathcal{U}[\mathbf{u}^K, \Phi^K]$ along the path $t \mapsto \psi_t^K(x)$. Indeed, one easily verifies (cf. [ENR20, Proposition 9]) that z_t^K and w_t^K are admissible in the sense of equations (15) and (16), i.e.

$$\begin{aligned}|u_t^K \circ \psi_t^K - u_s^K \circ \psi_s^K| &\leq \int_s^t z_r^K \circ \psi_r^K \, dr, \\ |u_{t+\tau}^K \circ \psi_{t+\tau}^K - u_t^K \circ \psi_t^K - u_{s+\tau}^K \circ \psi_{s+\tau}^K + u_s^K \circ \psi_s^K| &\leq \int_0^\tau \int_s^t w_{r+l}^K \circ \psi_{r+l}^K \, dl \, dr.\end{aligned}$$

Remark 4. For periodic boundary conditions we stick to the cubic interpolation definition on $t \in [t_{k-\frac{1}{2}}^K, t_{k+\frac{1}{2}}^K)$ for $k = 1, \dots, K$, with the convention $K \triangleq 0, K+1 \triangleq 1$ and $[t_{K-\frac{1}{2}}^K, t_{K+\frac{1}{2}}^K) = [t_{K-\frac{1}{2}}^K, 1] \cup [0, t_{\frac{1}{2}}^K)$.

Finally, we define the extension of the energy $\mathbf{F}^{\sigma,K}$ to a functional $\mathcal{F}^{\sigma,K}$ by

$$\mathcal{F}^{\sigma,K}[u] = \inf_{\Phi^K \in \mathcal{D}^K} \{ \mathbf{F}^{\sigma,K,D}[\mathbf{u}^K, \Phi^K] : \mathcal{U}[\mathbf{u}^K, \Phi^K] = u \}$$

if there exists such \mathbf{u}^K, Φ^K and $+\infty$ else. The existence of the infimum follows from the continuity of the constraint $\mathcal{U}[\mathbf{u}^K, \Phi^K] = u$ w.r.t. Φ^K (cf. [ENR20, Lemma 11]).

6 Convergence of time discrete splines

In this section we study the convergence of extension of discrete regularized spline energy $\mathcal{F}^{\sigma,K}$ to continuous counterpart \mathcal{F}^σ and the convergence of time discrete minimizers to a time continuous minimizer in the sense of Mosco.

We prove the Mosco convergence of energy $\mathcal{F}^{\sigma,K}$ to \mathcal{F}^σ in $L^2((0,1) \times \Omega)$.

Theorem 2. (*Mosco-convergence of the discrete spline energies*) *Let $\sigma > 0$. Then the discrete spline energy $\{\mathcal{F}^{\sigma,K}\}_{K \in \mathbb{N}}$ converges to \mathcal{F}^σ in the sense of Mosco in the topology $L^2((0,1) \times \mathcal{I})$ for $K \rightarrow \infty$. In explicit*

- (i) *for every sequence $\{u^K \in L^2((0,1) \times \mathcal{I})\}_{K \in \mathbb{N}}$ which converges weakly to $u \in L^2((0,1) \times \mathcal{I})$ as $K \rightarrow \infty$ it holds $\liminf_{K \rightarrow \infty} \mathcal{F}^{\sigma,K}[u^K] \geq \mathcal{F}^\sigma[u]$,*
- (ii) *for every $u \in L^2((0,1) \times \mathcal{I})$ there exists a sequence $\{u^K\}_{K \in \mathbb{N}}$ such that $u^K \rightarrow u$ in $L^2((0,1) \times \mathcal{I})$ as $K \rightarrow \infty$ and $\limsup_{K \rightarrow \infty} \mathcal{F}^{\sigma,K}[u^K] \leq \mathcal{F}^\sigma[u]$.*

Remark 5. *The above result holds for any choice of W_D satisfying assumption (W1)–(W3) from [EKP⁺21], though we restrict ourselves to the special case $W_D = |A^{sym} - \mathbb{1}|^2$.*

Remark 6. *In the case of periodic boundary conditions, the same applies in the topology $L^2(\mathbb{S}^1 \times \mathcal{I})$. The proof requires minor alterations implied by already indicated changes in energy and interpolation.*

Proof of the lim inf estimate.

Suppose we have a sequence $\{u^K \in L^2((0,1), \mathcal{I})\}_{K \in \mathbb{N}}$ such that $u^K \rightharpoonup u$ in that space as $K \rightarrow \infty$, and we suppose that $\mathcal{F}^{\sigma,K}[u^K] < \overline{\mathcal{F}} < \infty$. By definition for every K large enough an image vector $\mathbf{u}^K \in \mathcal{I}^{K+1}$ and a corresponding optimal vector of deformations $\Phi^K \in \mathcal{D}^K$ exist, such that

$$u^K = \mathcal{U}[\mathbf{u}^K, \Phi^K], \quad \mathcal{F}^{\sigma,K}[u^K] = \mathbf{F}^{\sigma,K,D}[\mathbf{u}^K, \Phi^K].$$

For the image vectors \mathbf{u}^K and the deformation vectors Φ^K we define the discrete velocity and acceleration quantities as in Section 4 and their extensions as in Section 5. Using Lemma 1 we have

$$\max_{k=1,\dots,K} \|\phi_k^K - \mathbb{1}\|_{C^{1,\alpha}(\overline{\Omega})} \leq CK^{-\frac{1}{2}}, \quad (36)$$

$$\max_{k=1,\dots,K-1} \|a_k^K\|_{C^{1,\alpha}(\overline{\Omega})} \leq CK^{\frac{1}{2}}, \quad (37)$$

which implies that y_k^K is invertible for any $k = 0, \dots, K$ and any K large enough. Thus, we are able to define all the temporal extended quantities introduced in the previous section. Furthermore, $y_k^K(t, \cdot)$ is uniformly in $C^{1,\alpha}(\overline{\Omega}, \overline{\Omega})$ and by [BHS05, Theorem 2.1] the same holds for $x_k^K(t, \cdot)$ with an estimate

$$\|x_k^K(t, \cdot)\|_{C^{1,\alpha}(\overline{\Omega})} \leq C(1 + \max_{k=1,\dots,K} \|\phi_k^K - \mathbb{1}\|_{C^{1,\alpha}(\overline{\Omega})}). \quad (38)$$

In what follows, the quantities \hat{z}_k^K and \hat{w}_k^K are time discrete quantities from Section 4, while z_t^K and w_t^K are their time extensions from Section 5. The estimate (38) together with locally Lipschitz property of the determinant function gives

$$\begin{aligned} \lim_{K \rightarrow \infty} \int_0^1 \int_{\Omega} (w_t^K)^2 dx dt &= \lim_{K \rightarrow \infty} \sum_{k=1}^{K-1} \int_{\Omega} \int_{t_{k-\frac{1}{2}}^K}^{t_{k+\frac{1}{2}}^K} (\hat{w}_k^K(x_k^K(t, x)))^2 dt dx \\ &= \lim_{K \rightarrow \infty} \sum_{k=1}^{K-1} \int_{\Omega} \int_{t_{k-\frac{1}{2}}^K}^{t_{k+\frac{1}{2}}^K} (\hat{w}_k^K(x))^2 \det(Dy_k^K(t, x)) dt dx \\ &= \lim_{K \rightarrow \infty} \frac{1}{K} \sum_{k=1}^{K-1} \int_{\Omega} (\hat{w}_k^K)^2 dx. \end{aligned}$$

Here we used the Riemannian approximation of the integral. Using the same ideas, with approximation of the time integrals first in the initial and then in the final points of intervals $[t_{k-\frac{1}{2}}^K, t_{k+\frac{1}{2}}^K]$ we have

$$\lim_{K \rightarrow \infty} \int_0^1 \int_{\Omega} (z_t^K)^2 dx dt = \lim_{K \rightarrow \infty} \frac{1}{K} \sum_{k=1}^K \int_{\Omega} (\hat{z}_k^K)^2 dx.$$

This implies the uniform boundedness of z^K and w^K in $L^2((0, 1) \times \Omega)$ and by reflexivity the existence of weakly convergent subsequences (with the same labelling) to z and w , respectively. Then by weak lower semi-continuity we have

$$\begin{aligned} \|z\|_{L^2((0,1) \times \Omega)}^2 &\leq \liminf_{K \rightarrow \infty} \|z^K\|_{L^2((0,1) \times \Omega)}^2, \\ \|w\|_{L^2((0,1) \times \Omega)}^2 &\leq \liminf_{K \rightarrow \infty} \|w^K\|_{L^2((0,1) \times \Omega)}^2. \end{aligned}$$

Using Korn's and Poincaré's inequality we get

$$\begin{aligned} \int_0^1 \int_{\Omega} (a^K)^2 dx dt &= \sum_{k=1}^{K-1} \int_{t_{k-\frac{1}{2}}^K}^{t_{k+\frac{1}{2}}^K} \int_{\Omega} (a_k^K(t, x))^2 dx dt \leq \frac{C}{K} \sum_{k=1}^{K-1} \int_{\Omega} W_A(Da_k^K) dx \leq C\overline{\mathcal{F}}, \\ \int_0^1 \int_{\Omega} |D^m a^K|^2 dx dt &= \sum_{k=1}^{K-1} \int_{t_{k-\frac{1}{2}}^K}^{t_{k+\frac{1}{2}}^K} \int_{\Omega} |D^m a_k^K|^2 dx dt \leq \sum_{k=1}^{K-1} \frac{1}{K} \int_{\Omega} |D^m a_k^K|^2 dx \leq C\overline{\mathcal{F}}. \end{aligned}$$

The analogous estimates hold for v^K and $D^m v^K$, by using approximation of Riemannian integral at the initial and final points of intervals of size K^{-1} . Hence, we have that v^K and a^K are uniformly bounded in $L^2((0, 1), \mathcal{V})$ and they have corresponding weak limits v and a in that space.

Furthermore, we compute the Taylor expansion of $W_A((t - t_{k-\frac{1}{2}}^K)^2 Da_k^K)$ at $t_{k-\frac{1}{2}}^K$, evaluated at $t = t_{k+\frac{1}{2}}^K$ to get

$$\frac{1}{K^4} W_A(Da_k^K) = \frac{1}{2K^4} D^2 W_A(\mathbf{0})(Da_k^K, Da_k^K) + r_{a,k}^K = \frac{1}{K^4} \text{tr}(\varepsilon[a_k^K]^2) + r_{a,k}^K. \quad (39)$$

For the remainder term we have $r_{a,k}^K = \mathcal{O}(K^{-6}|Da_k^K|^3)$ and by using Lemma 1 and (37)

$$\sum_{k=1}^{K-1} K^3 \int_{\Omega} r_{a,k}^K dx \leq \frac{C}{K^2} \max_{k=1, \dots, K-1} \|a_k^K\|_{C^1(\overline{\Omega})} \frac{1}{K} \sum_{k=1}^{K-1} \|a_k^K\|_{H^m(\Omega)}^2 \leq CK^{-\frac{3}{2}} \overline{\mathcal{F}}. \quad (40)$$

Then we use weak lower semi-continuity of the energy to write

$$\begin{aligned}
\liminf_{K \rightarrow \infty} \frac{1}{K} \sum_{k=1}^{K-1} \int_{\Omega} W_A(Da_k^K) + \gamma |D^m a_k^K|^2 dx &= \liminf_{K \rightarrow \infty} \frac{1}{K} \sum_{k=1}^{K-1} \int_{\Omega} \text{tr}(\varepsilon[a_k^K]^2) + \gamma |D^m a_k^K|^2 dx \\
&= \liminf_{K \rightarrow \infty} \int_0^1 \int_{\Omega} \text{tr}(\varepsilon[a^K]^2) + \gamma |D^m a^K|^2 dx dt \\
&\geq \int_0^1 \int_{\Omega} \text{tr}(\varepsilon[a]^2) + \gamma |D^m a|^2 dx dt.
\end{aligned}$$

Analogous Taylor expansion arguments give

$$\begin{aligned}
\liminf_{K \rightarrow \infty} K \sum_{k=1}^K \int_{\Omega} W_D(D\phi_k^K) + \gamma |D^m \phi_k^K|^2 dx &= \liminf_{K \rightarrow \infty} \int_0^1 \int_{\Omega} \text{tr}(\varepsilon[v^K]^2) + \gamma |D^m v^K|^2 dx dt \\
&\geq \int_0^1 \int_{\Omega} \text{tr}(\varepsilon[v]^2) + \gamma |D^m v|^2 dx dt.
\end{aligned}$$

Finally, let us observe that by using (38) (cf. also [Fio17, Proposition 1.2.4, 1.2.7]) we have

$$\|\tilde{v}_t^K\|_{C^{1,\alpha}(\bar{\Omega})} \leq C \|v_t^K\|_{C^{1,\alpha}(\bar{\Omega})} (1 + \max_{k=1,\dots,K} \|\phi_k^K - \mathbb{1}\|_{C^{1,\alpha}(\bar{\Omega})}) \quad (41)$$

$$\|\tilde{a}_t^K\|_{C^{1,\alpha}(\bar{\Omega})} \leq C \|a_t^K\|_{C^{1,\alpha}(\bar{\Omega})} (1 + \max_{k=1,\dots,K} \|\phi_k^K - \mathbb{1}\|_{C^{1,\alpha}(\bar{\Omega})}), \quad (42)$$

where \tilde{v}_t^K and \tilde{a}_t^K are introduced in (34).

We are left to show that the limit objects v, a, z, w are indeed corresponding quantities for the image curve u .

First we observe that we have the uniform boundedness of \tilde{v}^K in $L^2((0,1), \mathcal{V})$ and in $L^2((0,1), C^{1,\alpha}(\bar{\Omega}, \mathbb{R}^d))$ by (41). Then by [ENR20, Theorem 6] and Hölder's inequality we can infer that $\{\psi^K\}_{K \in \mathbb{N}}$ is uniformly bounded in $C^{0,\frac{1}{2}}([0,1], C^{1,\alpha}(\bar{\Omega}, \bar{\Omega}))$. Furthermore, by compact embedding of Hölder spaces, we have for some $\min\{\frac{1}{2}, \alpha\} > \beta > 0$ that $\psi^K \rightarrow \psi$ in $C^{0,\beta}([0,1], C^{1,\beta}(\bar{\Omega}, \bar{\Omega}))$. To show that ψ is indeed the solution corresponding to v , we consider $\tilde{\psi}^K$, the solutions corresponding to v^K . By weak continuity of the solution operator mapping velocities to the flows [ENR20, Theorem 6] we have $\tilde{\psi}^K \rightarrow \tilde{\psi}$ in $C^0([0,1] \times \bar{\Omega})$. Furthermore by [ENR20, Remark 7] we have the Lipschitz continuity of the solution operator and using the spatial Lipschitz property of v_k^K together with (36) we have $\psi^K - \tilde{\psi}^K \rightarrow 0$ in $C^0([0,1] \times \bar{\Omega})$ which finally confirms $\psi = \tilde{\psi}$.

To show that the equation $\ddot{\psi}_t = a_t \circ \psi_t$ is satisfied first observe that the equation $\ddot{\psi}_t^K = \tilde{a}_t^K \circ \psi_t^K$ ensures the uniform boundedness of $\ddot{\psi}^K$ in the space $L^2((0,1), C^{1,\alpha}(\bar{\Omega}, \bar{\Omega}))$. To this end we used the uniform boundedness of \tilde{a}^K in $L^2((0,1), C^{1,\alpha}(\bar{\Omega}, \bar{\Omega}))$ (cf. (42)) and ψ^K in $C^0([0,1], C^{1,\alpha}(\bar{\Omega}, \bar{\Omega}))$. This implies that $\ddot{\psi}^K$ is uniformly bounded in $H^1((0,1), C^{1,\alpha}(\bar{\Omega}, \bar{\Omega}))$ and converges weakly to $\ddot{\psi} \in H^1((0,1), C^{1,\beta}(\bar{\Omega}, \bar{\Omega}))$ and strongly in $C^{0,\beta}([0,1], C^{1,\beta}(\bar{\Omega}, \bar{\Omega}))$ for $\min\{\frac{1}{2}, \alpha\} > \beta > 0$. Thus, $\ddot{\psi} = \ddot{\psi}$ since we already established that $\psi^K \rightarrow \psi$ in $C^{0,\beta}([0,1], C^{1,\beta}(\bar{\Omega}, \bar{\Omega}))$. Altogether, we have that $\psi \in H^2((0,1), C^{1,\beta}(\bar{\Omega}, \bar{\Omega}))$ and

$$\left| \int_{\Omega} \int_0^1 \left(\tilde{a}_t^K \circ \psi_t^K(x) - \ddot{\psi}_t(x) \right) \theta_t(x) dt dx \right| \rightarrow 0,$$

for all $\theta \in C_c^\infty((0,1) \times \Omega)$. Hence, it suffices to verify $\tilde{a}^K \circ \psi^K \rightharpoonup a \circ \psi$ in $L^2((0,1) \times \Omega)$. Since we already have $a^K \circ \psi^K \rightharpoonup a \circ \psi$ in $L^2((0,1) \times \Omega)$, we conclude the proof by checking that $\tilde{a}^K \circ \psi^K - a^K \circ \psi^K \rightarrow 0$

in $L^2((0,1), C^0(\overline{\Omega}, \overline{\Omega}))$. Indeed

$$\begin{aligned}
\|\tilde{a}^K \circ \psi^K - a^K \circ \psi^K\|_{L^2((0,1), C^0(\overline{\Omega}))}^2 &\leq C \int_0^1 \|\tilde{a}_t^K \circ \psi_t^K - a_t^K \circ \psi_t^K\|_{C^0(\overline{\Omega})}^2 dt \\
&\leq C \sum_{k=1}^K \int_{t_{k-1}^K}^{t_k^K} \|\tilde{a}_t^K \circ \psi_t^K - a_t^K \circ \psi_t^K\|_{C^0(\overline{\Omega})}^2 dt \\
&\leq C \sum_{k=1}^K \int_{t_{k-1}^K}^{t_k^K} \|a_k^K(t, \cdot)\|_{C^1(\overline{\Omega})}^2 \|y_k^K(t, \cdot) - \mathbb{1}\|_{C^0(\overline{\Omega})}^2 dt \\
&\leq C \|a^K\|_{L^2((0,1), C^1(\overline{\Omega}))}^2 \max_k \|\phi_k^K - \mathbb{1}\|_{C^0(\overline{\Omega})}^2 \\
&\leq CK^{-1} \|a^K\|_{L^2((0,1), C^1(\overline{\Omega}))}^2,
\end{aligned}$$

where we used the Lipschitz property of a_t^K , the transformation formula and finally (36).

In order to show that z and w are indeed scalar weak material derivatives of u , first observe that from the weak convergence $u^K \rightharpoonup u$ and the strong convergence $\psi^K \rightarrow \psi$ by similar approximation arguments as for (32) we obtain $u^K \circ \psi^K \rightharpoonup u \circ \psi$ in $L^2((0,1) \times \Omega)$ and analogously $z^K \circ \psi^K \rightharpoonup z \circ \psi$ and $w^K \circ \psi^K \rightharpoonup w \circ \psi$. Next, note that for $s, t \in [0,1]$ we obtain

$$\begin{aligned}
\int_{\Omega} (u_t^K \circ \psi_t^K - u_s^K \circ \psi_s^K)^2 dx &\leq |t-s| \left| \int_s^t \int_{\Omega} (z_r^K \circ \psi_r^K)^2 dx dr \right| \\
&\leq C |t-s| \|z^K\|_{L^2((0,1) \times \Omega)}^2,
\end{aligned}$$

where we used Hölder's inequality, the transformation formula and uniform boundedness of $(\psi^K)^{-1}$. Thus, $\{u^K \circ \psi^K\}_{K \in \mathbb{N}}$ is a subset of

$$A_{\frac{1}{2}, L} := \{u \in L^2((0,1), \mathcal{I}) : \|u_t - u_s\|_{L^2(\Omega)} \leq L|t-s|^{\frac{1}{2}}\},$$

for some finite $L > 0$. Then, by the weak closedness of $A_{\frac{1}{2}, L}$ we obtain $u \circ \psi \in A_{\frac{1}{2}, L}$. The functional $u \mapsto \int_{\Omega} |u_t(x) - u_s(x)| dx$ is continuous because the point evaluation in time is continuous and convex on $A_{\frac{1}{2}, L}$ which implies weak lower semi-continuity and we obtain

$$\begin{aligned}
\int_{\Omega} |u_t \circ \psi_t - u_s \circ \psi_s| dx &\leq \liminf_{K \rightarrow \infty} \int_{\Omega} |u_t^K \circ \psi_t^K - u_s^K \circ \psi_s^K| dx \\
&\leq \liminf_{K \rightarrow \infty} \int_{\Omega} \int_s^t z_r^K \circ \psi_r^K dr dx \\
&= \int_{\Omega} \int_s^t z_r \circ \psi_r dr dx.
\end{aligned}$$

We prove that w is the second scalar weak material derivative for u in an analogous way. This finally finishes the proof of the lim inf-inequality.

As a preparatory step for the proof of the lim sup-estimate we state a corollary of the preceding proof.

Proposition 4. *For $u \in L^2([0,1], \mathcal{I})$ with $\mathcal{F}^\sigma[u] < \infty$ there exists an optimal tuple $(v, a, z, w) \in \mathcal{C}[u]$ such that*

$$\mathcal{F}^\sigma[u] = \int_0^1 L[a, a] + \frac{1}{\delta} w^2 + \sigma \left(L[v, v] + \frac{1}{\delta} z^2 \right) dx dt.$$

Proof. The functional \mathcal{F}^σ is coercive by Korn's inequality and Gagliardo-Nirenberg interpolation estimate and it is clearly weak-lower semi-continuous. Since $\mathcal{C}[u]$ is a subset of a reflexive Banach space, then we just have to show weak closedness of the set. This is verified as above. \square

Proof of the lim sup estimate and the construction of a recovery sequence.

Consider an image curve $u \in L^2([0, 1], \mathcal{I})$ with finite regularized spline energy. Then, the previous proposition guarantees the existence of an associated optimal velocity field, an acceleration field and the first and second order weak material derivatives, denoted by $(v, a, z, w) \in \mathcal{C}[u]$, respectively, i.e.

$$\mathcal{F}^\sigma[u] = \int_0^1 \int_\Omega L[a, a] + \frac{1}{\delta} w^2 + \sigma \left(L[v, v] + \frac{1}{\delta} z^2 \right) dx dt.$$

We define

$$\phi_k^K := \psi_{t_{k-1}^K, t_k^K} = \psi_{t_k^K} \circ \psi_{t_{k-1}^K}^{-1}, \quad k = 1, \dots, K, \quad (43)$$

where ψ_t is the flow associated with velocity v and $\psi_0 = \mathbb{1}$. We have

$$\begin{aligned} \max_k \|\phi_k^K - \mathbb{1}\|_{C^1(\overline{\Omega})} &\leq \sup_{|s-t| \leq \frac{1}{K}} \|\psi_{s,t} - \mathbb{1}\|_{C^1(\overline{\Omega})} \\ &\leq \sup_{|t-s| \leq K^{-1}} C \left| \int_s^t \|v_r \circ \psi_r\|_{H^m(\Omega)} dr \right| \\ &\leq \sup_{|t-s| \leq K^{-1}} C \left| \int_s^t \|v_r\|_{H^m(\Omega)} dr \right| \\ &\leq CK^{-\frac{1}{2}} \sup_{|t-s| \leq K^{-1}} \left| \int_s^t \|v_r\|_{H^m(\Omega)}^2 dr \right|^{\frac{1}{2}} \leq CK^{-\frac{1}{2}} \sqrt{\mathcal{F}^\sigma[u]}, \end{aligned} \quad (44)$$

by Lemma 1 and Cauchy's inequality. For the second inequality we used [BV17, Lemma 3.5] which states that

$$\|v_r \circ \psi_r\|_{H^m(\Omega)} \leq C \|v_r\|_{H^m(\Omega)}. \quad (45)$$

Thereby, for K large enough we have $\Phi \in \mathcal{D}^K$ and we are in a position to define

$$u^K = \mathcal{U}[\mathbf{u}^K, \Phi^K], \quad \mathbf{u}^K(\cdot) = (u(t_0^K, \cdot), \dots, u(t_K^K, \cdot)),$$

where the point time evaluation is possible since $u \in C^0([0, 1], \mathcal{I})$ (cf. [EKP⁺21, Remark 1]).

In what follows we present more detailed arguments for the second order terms, while the arguments for the first order terms follow as in [ENR20, Theorem 14].

First, we are able to connect the discrete and the continuous second order material derivative by

$$\begin{aligned}
& \int_{\Omega} |u_{k+1}^K \circ \phi_{k+1}^K \circ \phi_k^K - 2u_k^K \circ \phi_k^K + u_{k-1}^K|^2 dx \\
&= \int_{\Omega} |u_{t_{k+1}^K} \circ \psi_{t_{k-1}^K, t_{k+1}^K} - 2u_{t_k^K} \circ \psi_{t_{k-1}^K, t_k^K} + u_{t_{k-1}^K}|^2 dx \\
&= \int_{\Omega} |u_{t_{k+1}^K} \circ \psi_{t_{k+1}^K} - 2u_{t_k^K} \circ \psi_{t_k^K} + u_{t_{k-1}^K} \circ \psi_{t_{k-1}^K}|^2 \det(D\psi_{t_{k-1}^K}) dx \\
&\leq \int_{\Omega} \left(\int_{t_{k-1}^K}^{t_k^K} \int_0^{\frac{1}{K}} w_{r+s} \circ \psi_{r+s} dr ds \right)^2 \det(D\psi_{t_{k-1}^K}) dx \\
&\leq \frac{1}{K^2} \int_0^{\frac{1}{K}} \int_{t_{k-1}^K}^{t_k^K} \int_{\Omega} w_{r+s}^2 \det(D\psi_{r+s, t_{k-1}^K}) dx ds dr \\
&\leq \frac{1}{K^2} (1 + CK^{-\frac{1}{2}}) \int_0^{\frac{1}{K}} \int_{t_{k-1}^K}^{t_k^K} \int_{\Omega} w_{r+s}^2 dx ds dr.
\end{aligned}$$

Here, we first used (43) and the transformation formula for the first and the second equality, respectively, then the definition of the second order material derivative (11) for the first inequality, and the Cauchy-Schwarz inequality and (44) in the last two estimates. Summing the above expressions over $k = 1, \dots, K-1$, we obtain

$$\begin{aligned}
K^3 \sum_{k=1}^{K-1} \int_{\Omega} |u_{k+1}^K \circ \phi_{k+1}^K \circ \phi_k^K - 2u_k^K \circ \phi_k^K + u_{k-1}^K|^2 dx &\leq K(1 + CK^{-\frac{1}{2}}) \int_0^{\frac{1}{K}} \int_0^{1-\frac{1}{K}} \int_{\Omega} w_{r+s}^2 dx ds dr \\
&\leq K(1 + CK^{-\frac{1}{2}}) \int_0^{\frac{1}{K}} \int_0^1 \int_{\Omega} w_t^2 dx dt dr \\
&\leq (1 + CK^{-\frac{1}{2}}) \int_0^1 \int_{\Omega} w_t^2 dx dt. \tag{46}
\end{aligned}$$

Next, we express a_k^K in terms of a :

$$\begin{aligned}
a_k^K &= K^2(\phi_{k+1}^K \circ \phi_k^K - 2\phi_k^K + \mathbb{1}) \\
&= K^2(\psi_{t_{k-1}^K, t_{k+1}^K} - 2\psi_{t_{k-1}^K, t_k^K} + \psi_{t_{k-1}^K, t_{k-1}^K}) \\
&= K^2 \left(\int_{t_k^K}^{t_{k+1}^K} \dot{\psi}_t \circ \psi_{t_k^K}^{-1} dt - \int_{t_{k-1}^K}^{t_k^K} \dot{\psi}_t \circ \psi_{t_{k-1}^K}^{-1} dt \right) \\
&= K^2 \left(\int_{t_{k-1}^K}^{t_k^K} \int_0^{\frac{1}{K}} \ddot{\psi}_{t+\tau} \circ \psi_{t_{k-1}^K}^{-1} d\tau dt \right) \\
&= K^2 \left(\int_{t_{k-1}^K}^{t_k^K} \int_0^{\frac{1}{K}} a_{t+\tau} \circ \psi_{t_{k-1}^K, t+\tau} d\tau dt \right),
\end{aligned}$$

where in the second equality we used (43), and in the last equality (14). Then, using the Cauchy-Schwarz inequality and (45) we obtain the following estimate

$$\max_k \|a_k^K\|_{C^1(\bar{\Omega})} \leq CK^{\frac{1}{2}} \sup_{t \in [0,1], 0 < \tau \leq K^{-1}} \left| \int_t^{t+2\tau} \|a_s\|_{H^m(\Omega)}^2 ds \right|^{\frac{1}{2}}. \tag{47}$$

The same Taylor expansion argument as in (39) and (40) now implies, together with (47)

$$\int_{\Omega} W_A(Da_k^K) + \gamma |D^m a_k^K|^2 dx \leq \int_{\Omega} L[a_k^K, a_k^K] dx + CK^{-\frac{3}{2}} \sqrt{\mathcal{F}\sigma[u]}. \quad (48)$$

Applying Jensen's inequality twice on L , and taking into account the above connection between a_k^K and a gives

$$\begin{aligned} \int_{\Omega} L[a_k^K, a_k^K] dx &= \int_{\Omega} K^4 L \left[\int_{t_{k-1}^K}^{t_k^K} \int_0^{\frac{1}{K}} a_{t+\tau} \circ \psi_{t_{k-1}^K, t+\tau} d\tau dt, \right. \\ &\quad \left. \int_{t_{k-1}^K}^{t_k^K} \int_0^{\frac{1}{K}} a_{t+\tau} \circ \psi_{t_{k-1}^K, t+\tau} d\tau dt \right] dx \\ &\leq \int_{\Omega} K^2 \int_{t_{k-1}^K}^{t_k^K} \int_0^{\frac{1}{K}} L[a_{t+\tau} \circ \psi_{t_{k-1}^K, t+\tau} d\tau dt, \\ &\quad a_{t+\tau} \circ \psi_{t_{k-1}^K, t+\tau} d\tau dt] dx. \end{aligned}$$

We now estimate the summands of L individually. For the first term we use that $|tr(AB)| \leq |tr(A)| + |trA(B - \mathbb{1})|$, (44) and transformation rule to get

$$\begin{aligned} &\int_{\Omega} \int_{t_{k-1}^K}^{t_k^K} \int_0^{\frac{1}{K}} tr \left(\varepsilon[a_{t+\tau} \circ \psi_{t_{k-1}^K, t+\tau}]^2 \right) d\tau dt dx \\ &\leq \int_{\Omega} \int_{t_{k-1}^K}^{t_k^K} \int_0^{\frac{1}{K}} tr \left((\varepsilon[a_{t+\tau}] \circ \psi_{t_{k-1}^K, t+\tau})^2 \right) tr \left((\varepsilon[a_{t+\tau}] \circ \psi_{t_{k-1}^K, t+\tau})^2 (\varepsilon[\psi_{t_{k-1}^K, t+\tau}]^2 - \mathbb{1}) \right) d\tau dt dx \\ &\leq \int_{\Omega} \int_{t_{k-1}^K}^{t_k^K} \int_0^{\frac{1}{K}} tr \left(\varepsilon[a_{t+\tau}]^2 \right) + CK^{-\frac{1}{2}} \|a_{t+\tau}\|_{H^m(\Omega)}^2 d\tau dt dx. \end{aligned}$$

For the second term we use (45) and the fact for any $0 \leq \tilde{m} \leq m$ and $f \in H^m(\Omega, \mathbb{R}^d)$, $g \in H^{\tilde{m}}(\Omega, \mathbb{R}^d)$ we have $\|fg\|_{H^{\tilde{m}}(\Omega)} \leq C\|f\|_{H^m(\Omega)}\|g\|_{H^{\tilde{m}}(\Omega)}$ [IKT13, Lemma 2.3] to get

$$\int_{\Omega} |D^m(a_{t+\tau} \circ \psi_{t_{k-1}^K, t+\tau})| dx \leq \int_{\Omega} |D^{m-1}a_{t+\tau} \circ \psi_{t_{k-1}^K, t+\tau}| dx + CK^{-\frac{1}{2}} \|a_{t+\tau}\|_{H^m(\Omega)},$$

and iterating this argument and using the transformation formula we have

$$\int_{\Omega} \int_{t_{k-1}^K}^{t_k^K} \int_0^{\frac{1}{K}} |D^m(a_{t+\tau} \circ \psi_{t_{k-1}^K, t+\tau})|^2 d\tau dt dx \leq \int_{t_{k-1}^K}^{t_k^K} \int_0^{\frac{1}{K}} |a_{t+\tau}|_{H^m(\Omega)}^2 + CK^{-\frac{1}{2}} \|a_{t+\tau}\|_{H^m(\Omega)}^2 d\tau dt.$$

Alltogether with (47) and (48) we have

$$\begin{aligned} \frac{1}{K} \sum_{k=1}^{K-1} \int_{\Omega} W_A(Da_k^K) + \gamma |D^m a_k^K|^2 &\leq K \int_0^{\frac{1}{K}} \int_0^{1-\frac{1}{K}} \int_{\Omega} L[a_{t+\tau}, a_{t+\tau}] + \mathcal{O}(K^{-\frac{1}{2}}) dt d\tau \\ &\leq \int_0^1 \int_{\Omega} L[a_t, a_t] + \mathcal{O}(K^{-\frac{1}{2}}) dt, \end{aligned}$$

which together with (46) gives

$$\mathcal{F}^K[u^K] \leq \mathcal{F}[u] + \mathcal{O}(K^{-\frac{1}{2}}).$$

This readily implies the lim sup-inequality for the pure spline part of the functional $\mathcal{F}^{\sigma,K}$.

Following analogous steps as above, we can fully repeat the procedure from [ENR20, Theorem 14] to obtain the estimate for the lower order path energy

$$\mathcal{E}^K[u^K] \leq \mathcal{E}[u] + \mathcal{O}(K^{-\frac{1}{2}}),$$

which finally proves the lim sup-inequality.

We are left to show that $u^K \rightarrow u$ in $L^2((0,1) \times \Omega)$ as $K \rightarrow \infty$. To this end we define the discrete flow ψ^K as in Section 5 and write

$$\begin{aligned} & \int_0^1 \int_{\Omega} |u_s \circ \psi_s - u_s^K \circ \psi_s^K|^2 dx ds \\ &= \int_{\Omega} \sum_{k=1}^{K-1} \int_{t_{k-\frac{1}{2}}^K}^{t_{k+\frac{1}{2}}^K} |u_s \circ \psi_s - u_s^K \circ \psi_s^K|^2 ds + \int_0^{t_{\frac{1}{2}}^K} |u_s \circ \psi_s - u_s^K \circ \psi_s^K|^2 ds \\ & \quad + \int_{t_{K-\frac{1}{2}}^K}^1 |u_s \circ \psi_s - u_s^K \circ \psi_s^K|^2 ds dx \end{aligned}$$

We show the estimates for the summands in the first term on the right hand side, while others are estimated analogously. Using the definition of the image extension (33) and Young's inequality we have that for every $k = 1, \dots, K-1$

$$\begin{aligned} & \frac{1}{4} \int_{t_{k-\frac{1}{2}}^K}^{t_{k+\frac{1}{2}}^K} \int_{\Omega} |u_s \circ \psi_s - u_s^K \circ \psi_s^K|^2 dx ds \\ & \leq \int_{\Omega} \int_{t_{k-\frac{1}{2}}^K}^{t_{k+\frac{1}{2}}^K} |u_s \circ \psi_s - u_{t_{k-\frac{1}{2}}^K} \circ \psi_{t_{k-\frac{1}{2}}^K}|^2 + \left| u_{t_{k-\frac{1}{2}}^K} \circ \psi_{t_{k-\frac{1}{2}}^K} - \frac{1}{2}(u_{t_{k-1}^K} \circ \psi_{t_{k-1}^K} + u_{t_k^K} \circ \psi_{t_k^K}) \right|^2 \\ & \quad + \left| u_{t_k^K} \circ \psi_{t_k^K} - u_{t_{k-1}^K} \circ \psi_{t_{k-1}^K} \right|^2 + \left| u_{t_{k+1}^K} \circ \psi_{t_{k+1}^K} - 2u_{t_k^K} \circ \psi_{t_k^K} + u_{t_{k-1}^K} \circ \psi_{t_{k-1}^K} \right|^2 ds dx. \end{aligned}$$

For the first term we have

$$\begin{aligned} & \int_{t_{k-\frac{1}{2}}^K}^{t_{k+\frac{1}{2}}^K} \int_{\Omega} |u_s \circ \psi_s - u_{t_{k-\frac{1}{2}}^K} \circ \psi_{t_{k-\frac{1}{2}}^K}|^2 dx ds \leq \int_{t_{k-\frac{1}{2}}^K}^{t_{k+\frac{1}{2}}^K} \int_{\Omega} \left| \int_{t_{k-\frac{1}{2}}^K}^s z_r \circ \psi_r dr \right|^2 dx ds \\ & \leq K^{-1} \int_{t_{k-\frac{1}{2}}^K}^{t_{k+\frac{1}{2}}^K} \int_{\Omega} \int_{t_{k-\frac{1}{2}}^K}^{t_{k+\frac{1}{2}}^K} (z_r \circ \psi_r)^2 dr dx ds \\ & \leq K^{-2} \int_{\Omega} \int_{t_{k-\frac{1}{2}}^K}^{t_{k+\frac{1}{2}}^K} (z_r \circ \psi_r)^2 dr dx, \end{aligned}$$

where we used (15) and Cauchy-Schwarz inequality. The third term is estimated analogously, while the second, and analogously the fourth term, can be estimated from above by

$$\begin{aligned} & K^{-1} \int_{\Omega} \left| u_{t_{k-\frac{1}{2}}^K} \circ \psi_{t_{k-\frac{1}{2}}^K} - \frac{1}{2}(u_{t_{k-1}^K} \circ \psi_{t_{k-1}^K} + u_{t_k^K} \circ \psi_{t_k^K}) \right|^2 dx \leq K^{-1} \int_{\Omega} \left| \int_{t_{k-1}^K}^{t_k^K} \int_0^{\frac{1}{2K}} w_{r+\tau} \circ \psi_{r+\tau} d\tau dr \right|^2 dx \\ & \leq CK^{-3} \int_{\Omega} \int_{t_{k-1}^K}^{t_k^K} \int_0^{\frac{1}{2K}} (w_{r+\tau} \circ \psi_{r+\tau})^2 d\tau dr dx, \end{aligned}$$

where we once again used Cauchy-Schwarz inequality and (16). Altogether, we have

$$\begin{aligned} \|u_t \circ \psi_t - u_t^K \circ \psi_t^K\|_{L^2((0,1) \times \Omega)}^2 &\leq C \left(K^{-2} \|z_t \circ \psi_t\|_{L^2((0,1) \times \Omega)}^2 + K^{-4} \|w_t \circ \psi_t\|_{L^2((0,1) \times \Omega)}^2 \right) \\ &\leq C \left(K^{-2} \|z_t\|_{L^2((0,1) \times \Omega)}^2 + K^{-4} \|w_t\|_{L^2((0,1) \times \Omega)}^2 \right). \end{aligned}$$

Finally, we use that $\psi^K \rightarrow \psi$ in $C^0([0, 1] \times \overline{\Omega})$ and the approximation technique as in (32) to conclude the proof.

As a corollary of the previous theorem we are able to show the existence of the continuous time spline defined in Section 3. To this end, let $J \geq 2$ and $(t_1, \dots, t_J) \subset [0, 1] \cap \mathbb{Q}$ be a sequence of fixed times. Then for infinitely many $K \in \mathbb{N}$ one can choose $i_j^K := K \cdot t_j \in \mathbb{N}$ for all $j = 1, \dots, J$. Let $(u_j^I)_{j=0, \dots, J} \subseteq \mathcal{I}$ be the set of constraint images at the corresponding constraint times.

Theorem 3 (Convergence of discrete spline interpolations to continuous ones). *For every K that satisfies the above condition, let $u^K \in L^2([0, 1], \mathcal{I})$ be a minimizer of $\mathcal{F}^{\sigma, K}$ among the image curves satisfying $u^K = \mathcal{U}[\mathbf{u}^K, \Phi^K]$ with $u_{i_j^K}^K = u_j^I$ for all $j \in \{0, \dots, J\}$. Then a subsequence of $\{u^K\}_{K \in \mathbb{N}}$ converges weakly in $L^2([0, 1], \mathcal{I})$ to a minimizer of the continuous spline energy \mathcal{F}^σ as $K \rightarrow \infty$. This minimizer satisfies $u(t_j) = u_j^I$ for all $j \in \{0, \dots, J\}$ and the associated sequence of discrete energies converges to the minimal continuous spline energy.*

Proof. For $j = 1, \dots, J$ let $\eta^j : [0, 1] \rightarrow \mathbb{R}$ be smooth functions with $\eta^j(t_i) = \delta_{ij}$. We define a smooth interpolating curve of the fixed images $\tilde{u}(t) := \sum_{j=0}^J \eta^j(t) u_j^I$. Let $\tilde{\mathbf{u}}^K := (\tilde{u}(t_0^K), \tilde{u}(t_1^K), \dots, \tilde{u}(t_K^K))$ and define $\tilde{u}^K := \mathcal{U}[\tilde{\mathbf{u}}^K, \mathbf{1}^K]$. This image curve gives an admissible candidate for a minimizer of the functional $\mathcal{F}^{\sigma, K}$. Namely,

$$\begin{aligned} \mathcal{F}^{\sigma, K}[\tilde{u}^K] &\leq \mathbf{F}^{\sigma, K, D}[\tilde{\mathbf{u}}^K, \mathbf{1}^K] \\ &= \sigma K \sum_{k=0}^K \int_{\Omega} |\tilde{\mathbf{u}}_{k+1}^K - \tilde{\mathbf{u}}_k^K|^2 dx + K^3 \sum_{k=1}^{K-1} \int_{\Omega} |\tilde{\mathbf{u}}_{k+1}^K - 2\tilde{\mathbf{u}}_k^K + \tilde{\mathbf{u}}_{k-1}^K|^2 dx \\ &\leq C \left(\int_{\Omega} |\tilde{u}|_{H^1((0,1))}^2 + |\tilde{u}|_{H^2((0,1))}^2 dx + 1 \right), \end{aligned}$$

where the upper bound is independent of K . As defined above, let $\{u^K := \mathcal{U}[\mathbf{u}^K, \Phi^K]\}_{K \in \mathbb{N}}$, where \mathbf{u}^K, Φ^K are optimal pairs for the discrete spline (see Theorem 1). In particular, we have $\mathcal{F}^{\sigma, K}[u^K] = \mathbf{F}^{\sigma, K}[\mathbf{u}^K, \Phi^K] < \mathcal{F}$. As in (29) we show uniform boundedness of u_k^K in $L^2(\Omega)$. This further implies, together with boundedness of the deformations and the convergence of the discrete transport paths to the identity that u_t^K is uniformly bounded in $L^2(\Omega)$. Therefore, $\{u^K\}_{K \in \mathbb{N}}$ is uniformly bounded in $L^\infty([0, 1], \mathcal{I})$ and a subsequence converges weakly to some $u \in L^2([0, 1], \mathcal{I})$.

Now, we follow the usual argument and assume that there exists an image path $\hat{u} \in L^2([0, 1], \mathcal{I})$ with finite energy such that $\mathcal{F}^\sigma[\hat{u}] < \mathcal{F}^\sigma[u]$. By the limsup-part of Theorem 2 there exists a sequence $\{\hat{u}^K\}_{K \in \mathbb{N}} \subseteq L^2((0, 1), \mathcal{I})$ such that $\limsup_{K \rightarrow \infty} \mathcal{F}^{\sigma, K}[\hat{u}^K] \leq \mathcal{F}^\sigma[\hat{u}]$. Now, we apply the liminf-part of Theorem 2, thus obtaining

$$\mathcal{F}^\sigma[u] \leq \liminf_{K \rightarrow \infty} \mathcal{F}^{\sigma, K}[u^K] \leq \liminf_{K \rightarrow \infty} \mathcal{F}^{\sigma, K}[\hat{u}^K] \leq \mathcal{F}^\sigma[\hat{u}], \quad (49)$$

which is a contradiction to the above assumption. Hence, u minimizes the continuous spline energy over all admissible image curves and discrete spline energies converge to the limiting spline energy along a subsequence, i.e. $\lim_{K \rightarrow \infty} \mathcal{F}^{\sigma, K}[u^K] = \mathcal{F}^\sigma[u]$, which follows from (49) by using $\hat{u} = u$.

Finally, we show that $u_{t_j} = u_j^I$. To this end we introduce the piecewise constant interpolation

$$\bar{u}_t^K = \begin{cases} u_0^K, & t \in [0, t_{\frac{1}{2}}^K) \\ u_k^K, & t \in [t_{k-\frac{1}{2}}^K, t_{k+\frac{1}{2}}^K), \quad k = 1, \dots, K-1 \\ u_K^K, & t \in [t_{K-\frac{1}{2}}^K, 1], \end{cases}$$

and straightforwardly check that $u_t^K - \bar{u}_t^K \rightarrow 0$ in \mathcal{I} , uniformly in t . Together with $u_t^K \rightharpoonup u_t$ in \mathcal{I} for every $t \in [0, 1]$ which is showed by a trace theorem type argument (see [BER15, Theorem 4.1, (iv)]) we have the needed result since $\bar{u}_{t_j}^K = u_j^I$. \square

The analogous result for arbitrary $(t_1, \dots, t_J) \subset [0, 1]$ follows from density of \mathbb{Q} in $[0, 1]$. Let us remark that in light of Proposition 1 we have that we have that for optimal scalar quantities z, w it holds $z = |\hat{z}|$ and $w = |\hat{w}|$.

7 Fully Discrete Metamorphosis Splines

To implement splines for image metamorphosis numerically, we have to further discretize the space. Here, we present a model for c image channels and a two dimensional image domain $\Omega := [0, 1]^2$. At first, to avoid double warping in the second material derivative term (19) and to further increase the robustness of the model we explicitly introduce a vector valued material derivative $\bar{z} \in L^2((0, 1), L^2(\Omega, \mathbb{R}^C))$ and obtain a relaxation of (12):

$$\mathcal{F}^\sigma[u, \bar{z}] = \inf_{(v, a, z, w)} \int_0^1 \int_\Omega L[a, a] + \frac{1}{\delta} |w|^2 + \sigma(L[v, v] + \frac{1}{\delta} |\bar{z}|^2) + \frac{1}{\theta} |\bar{z} - \hat{z}|^2 \, dx \, dt,$$

with a penalty on the misfit of the new variable \bar{z} and the actual material derivative \hat{z} (cf. (4)), while w is the first material derivative of \bar{z} . To adapt the time discrete counterpart $\mathbf{F}^{\sigma, K}[\mathbf{u}, \bar{\mathbf{z}}]$ with $\bar{\mathbf{z}} = (\bar{z}_1, \dots, \bar{z}_K)$ we write

$$\begin{aligned} & \mathbf{F}^{\sigma, K, D}[\mathbf{u}, \bar{\mathbf{z}}, \Phi] \\ &= \int_\Omega \sum_{k=1}^{K-1} \frac{1}{K} (W_A(Da_k) + \gamma |D^m a_k|^2) + \frac{K}{\delta} |\bar{z}_{k+1} \circ \phi_k - \bar{z}_k|^2 + \sigma \left(\sum_{k=1}^K K W_D(D\phi_k) + K \gamma |D^m \phi_k|^2 + \frac{1}{\delta K} |\bar{z}_k|^2 \right) \\ &+ \sum_{k=1}^K \frac{1}{\theta K} |K(u_k \circ \phi_k - u_{k-1}) - \bar{z}_k|^2 \, dx, \end{aligned}$$

where $\bar{w}_k = K(\bar{z}_{k+1} \circ \phi_k - \bar{z}_k)$ is the discrete material derivative of \bar{z}_k , while $\hat{z}_k = K(u_k \circ \phi_k - u_{k-1})$ is the actual material derivative of u_k , with the corresponding second order derivative $(\hat{w}_k)_{k=1}^{K-1}$ given by (19).

For $M, N \geq 3$ we define the computational domain

$$\Omega_{MN} = \left\{ \frac{0}{M-1}, \frac{1}{M-1}, \dots, \frac{M-1}{M-1} \right\} \times \left\{ \frac{0}{N-1}, \frac{1}{N-1}, \dots, \frac{N-1}{N-1} \right\},$$

with discrete boundary $\partial\Omega_{MN} = \Omega_{MN} \cap \partial([0, 1]^2)$ and $\|\mathbf{u}\|_{L_{MN}^p}^p = \frac{1}{MN} \sum_{(i,j) \in \Omega_{MN}} \|\mathbf{u}(i, j)\|_p^p$. The discrete image space is $\mathcal{I}_{MN} := \{\mathbf{u} : \Omega_{MN} \rightarrow \mathbb{R}^C\}$ and the set of admissible deformations is

$$\mathcal{D}_{MN} = \{\phi : \Omega_{MN} \rightarrow [0, 1]^2, \phi = \mathbf{1} \text{ on } \partial\Omega_{MN}, \det(\nabla_{MN} \phi) > 0\},$$

where the discrete Jacobian operator of ϕ at $(i, j) \in \Omega_{MN}$ is defined as the forward finite difference operator with Neumann boundary conditions. Here and in the rest of the paper we used bold faced letters for fully discrete quantities. A spatial warping operator \mathbf{T} that approximates the pullback of an image channel $\mathbf{u}^j \circ \phi$ at a point $(x, y) \in \Omega_{MN}$ by

$$\mathbf{T}[\mathbf{u}^j, \phi](x, y) = \sum_{(i, j) \in \Omega_{MN}} s(\phi_1(x, y) - i) s(\phi_2(x, y) - j) \mathbf{u}^j(i, j),$$

where s is the third order B-spline interpolation kernel. This form of warping is also used for composition of deformations, i.e we define the fully discrete acceleration as an approximation of (18) by

$$\mathbf{a}_k^j := K^2(\mathbf{T}[\phi_{k+1}^j - \mathbf{1}, \phi_k] - (\phi_k^j - \mathbf{1})), \quad j = 1, 2.$$

In summary, the fully discrete spline energy in the metamorphosis model for a $(K + 1)$ -tuple $(\mathbf{u}_k)_{k=0}^K$ of discrete images and a K -tuple $(\bar{\mathbf{z}}_k)_{k=1}^K$ of discrete derivatives reads as

$$\begin{aligned} & \mathbf{F}_{MN}^{\sigma, K}[(\mathbf{u}_k)_{k=0}^K, (\bar{\mathbf{z}}_k)_{k=1}^K] \\ &= \inf_{\Phi \in \mathcal{D}_{MN}^K} \mathbf{F}_{MN}^{\sigma, K, D}[(\mathbf{u}_k)_{k=0}^K, (\bar{\mathbf{z}}_k)_{k=1}^K, (\phi_k)_{k=1}^K] \\ &= \inf_{\Phi \in \mathcal{D}_{MN}^K} \sum_{k=1}^{K-1} \frac{1}{K} \|W_A(\nabla_{MN} \mathbf{a}_k)\|_{L_{MN}^1} + \frac{K}{\delta} \mathbf{D}_{MN}^s[\bar{\mathbf{z}}_k, \bar{\mathbf{z}}_{k+1}, \phi_k] \\ & \quad + \sum_{k=1}^K \sigma \left(K \|W_D(\nabla_{MN} \phi_k)\|_{L_{MN}^1} + \frac{1}{\delta K} \|\bar{\mathbf{z}}_k\|_{L_{MN}^2}^2 \right) + \frac{1}{\theta K} \mathbf{D}_{MN}^g[\mathbf{u}_{k-1}, \mathbf{u}_k, \bar{\mathbf{z}}_k, \phi_k], \end{aligned}$$

where

$$\begin{aligned} \mathbf{D}_{MN}^s[\mathbf{z}, \tilde{\mathbf{z}}, \phi] &= \frac{1}{2c} \sum_{j=1}^c \|\mathbf{T}[\tilde{\mathbf{z}}^j, \phi] - \mathbf{z}^j\|_{L_{MN}^2}^2 \\ \mathbf{D}_{MN}^g[\mathbf{u}, \tilde{\mathbf{u}}, \mathbf{z}, \phi] &= \frac{1}{2c} \sum_{j=1}^c \|K(\mathbf{T}[\tilde{\mathbf{u}}^j, \phi] - \mathbf{u}^j) - \mathbf{z}^j\|_{L_{MN}^2}^2. \end{aligned}$$

While in the spatially continuous context the compactness induced by the H^m -seminorm is indispensable, in this fully discrete model grid dependent regularity is ensured by the use of cubic B-splines. Thus, we dropped the higher order Sobolev norm terms in this fully discrete model.

To improve the robustness of the overall optimization, we take into account a multiresolution strategy. In detail, on the coarse computational domain of size $M_L \times N_L$ with $M_L = 2^{-(L-1)}M$ and $N_L = 2^{-(L-1)}N$ for a given $L \geq 1$, a time discrete spline sequence $((\mathbf{u}_k)_{k=0}^K, (\bar{\mathbf{z}}_k)_{k=1}^K)$ is computed as minimizer of $\mathbf{F}_{M_L N_L}^{\sigma, K}$ subject to given fixed images $\mathbf{u}_{i_j} = \mathbf{u}_j^I$, $j = 1, \dots, J$. In subsequent prolongation steps, the width and the height of the computational domain are successively doubled and the initial deformations, images and derivatives are obtained via a bilinear interpolation of the preceding coarse scale solutions.

8 Numerical Optimization Using the iPALM Algorithm

In this section, we discuss the numerical solution of the above fully discrete variational problem based on the application of a variant of the inertial proximal alternating linearized minimization algorithm (iPALM, [PS16]). Following [EKP⁺21], to enhance the stability the warping operation is linearized

with respect to the deformation at $\phi^{[\beta]} \in \mathcal{D}_{MN}$ coming from the previous iteration which leads to the modified energies

$$\begin{aligned}\tilde{\mathbf{D}}_{MN}^s[\mathbf{z}, \tilde{\mathbf{z}}, \phi, \phi^{[\beta]}] &= \frac{1}{2c} \sum_{j=1}^c \left\| \mathbf{T}[\tilde{\mathbf{z}}^j, \phi^{[\beta]}] + \left\langle \Lambda_j(\mathbf{z}, \tilde{\mathbf{z}}, \phi^{[\beta]}), \phi - \phi^{[\beta]} \right\rangle - \mathbf{z}^j \right\|_{L_{MN}^2}^2 \\ \tilde{\mathbf{D}}_{MN}^g[\mathbf{u}, \tilde{\mathbf{u}}, \mathbf{z}, \phi, \phi^{[\beta]}] &= \frac{1}{2c} \sum_{j=1}^c \left\| K\mathbf{T}[\tilde{\mathbf{u}}^j, \phi^{[\beta]}] + \left\langle \Lambda_j(K\mathbf{u} + \mathbf{z}, K\tilde{\mathbf{u}}, \phi^{[\beta]}), \phi - \phi^{[\beta]} \right\rangle - (K\mathbf{u} + \mathbf{z}^j) \right\|_{L_{MN}^2}^2,\end{aligned}$$

based on the gradient

$$\Lambda_j(\mathbf{u}, \tilde{\mathbf{u}}, \phi^{[\beta]}) = \frac{1}{2}(\nabla \mathbf{T}[\tilde{\mathbf{u}}^j, \phi^{[\beta]}] + \nabla \mathbf{u}^j).$$

To further stabilize the computation, the Jacobian operator applied to the images is approximated using a Sobel filter. Here, $\langle \cdot, \cdot \rangle$ represent the pointwise product of the involved matrices. We use the proximal mapping of a functional $f : \mathcal{D}_{MN} \rightarrow (-\infty, \infty]$ for $\tau > 0$ given as

$$\text{prox}_\tau^f(x) := \underset{y \in \mathcal{D}_{MN}}{\text{argmin}} \left(\frac{\tau}{2} \|x - y\|_{L^2(\Omega)}^2 + f(y) \right).$$

Then, with the function values on $\partial\Omega_{MN}$ remaining unchanged, the proximal operator we are interested in is given by

$$\begin{aligned}& \text{prox}_{\frac{K}{\delta}}^{\tilde{\mathbf{D}}_{MN}^s + \frac{1}{K\theta}\tilde{\mathbf{D}}_{MN}^g}[\phi_k^t] \\ &= \left(\mathbf{1} + \frac{K}{c\tau\delta} \sum_{j=1}^c |\Lambda_j^s|^2 + \frac{1}{c\tau\theta K} \sum_{j=1}^c |\Lambda_j^g|^2 \right) \\ & \quad \left(\phi_k^t - \frac{K}{c\tau\delta} \sum_{j=1}^c \Lambda_j^s (\mathbf{T}[\bar{\mathbf{z}}_{k+1}^j, \phi_k^{[\beta]}] - (\Lambda_j^s)^T \phi_k^{[\beta]} - \bar{\mathbf{z}}_k^j) - \frac{1}{c\tau\theta K} \sum_{j=1}^c \Lambda_j^g (\mathbf{T}[K\mathbf{u}_k^j, \phi_k^{[\beta]}] - (\Lambda_j^g)^T \phi_k^{[\beta]} - K\mathbf{u}_{k-1}^j - \bar{\mathbf{z}}_k^j) \right),\end{aligned}$$

where $\Lambda_j^s := \Lambda(\bar{\mathbf{z}}_k^j, \bar{\mathbf{z}}_{k+1}^j, \phi_k^{[\beta]})$ and $\Lambda_j^g := \Lambda(K\mathbf{u}_{k-1}^j + \bar{\mathbf{z}}_k^j, K\mathbf{u}_k^j, \phi_k^{[\beta]})$. The first terms in both brackets are activated only for $k < K$.

In the l^{th} iteration of the algorithm for the minimization of the spline energy $\mathbf{F}_{MN}^{\sigma, K}$ the k^{th} path elements are updated as follows

$$\begin{aligned}\phi_k^{l,t} &= \phi_k^{[\beta,l]} - \frac{1}{L[\phi_k^{[l]}]} \nabla \phi_k \left(\sigma K \|W_D(\nabla_{MN} \phi_k^{[\beta,l]})\|_{L_{MN}^1} \frac{1}{K} \|W_A(\nabla_{MN} \mathbf{a}_k^{[\beta,l]}) + W_A(\nabla_{MN} \mathbf{a}_{k-1}^{[\beta,l]})\|_{L_{MN}^1} \right), \\ \phi_k^{[l+1]} &= \text{prox}_{\frac{K}{\delta}}^{\tilde{\mathbf{D}}_{MN}^s + \frac{1}{K\theta}\tilde{\mathbf{D}}_{MN}^g}[\phi_k^{l,t}], \\ \bar{\mathbf{z}}_k^{[l+1]} &= \bar{\mathbf{z}}_k^{[\beta,l]} - \frac{\nabla_{\bar{\mathbf{z}}_k} \mathbf{F}_{MN}^{\sigma, K, D}[\mathbf{u}^{[k,l]}, \bar{\mathbf{z}}^{[\beta,k,l]}, \phi^{[k+1,l]}]}{L[\bar{\mathbf{z}}_k^{[l]}]}, \\ \mathbf{u}_k^{[l+1]} &= \mathbf{u}_k^{[\beta,l]} - \frac{\nabla_{\mathbf{u}_k} \mathbf{F}_{MN}^{\sigma, K, D}[\mathbf{u}^{[\beta,k,l]}, \bar{\mathbf{z}}^{[k+1,l]}, \phi^{[k+1,l]}]}{L[\mathbf{u}_k^{[l]}]}.\end{aligned}$$

Here, we used the following notation for the extrapolation with $\beta > 0$ of the k^{th} path element in the l^{th} iteration step

$$\begin{aligned}h_k^{[\beta,l]} &= h_k^{[l]} + \beta(h_k^{[l]} - h_k^{[l-1]}), \\ h^{[k,l]} &= (h_{1,\dots,k-1}^{[l+1]}, h_{k,\dots,K}^{[l]}), \\ h^{[\beta,k,l]} &= (h_1^{[l+1]}, \dots, h_{k-1}^{[l+1]}, h_k^{[\beta,l]}, h_{k+1}^{[l]}, \dots, h_K^{[l]}),\end{aligned}$$

while the acceleration $\mathbf{a}^{[\beta,l]}$ is computed with correspondingly updated $\phi^{[\beta,l]}$ values. Furthermore, we denote by $L[h]$ the Lipschitz constant of the gradient of the function h , which is determined by backtracking.

9 Applications

In what follows, we investigate and discuss qualitative properties of the spline interpolation in the space of images, being aware that the superior temporal smoothness of this interpolation is difficult to show with series of still images. For all the examples we use 5 levels in the multi-levels approach and $\beta = \frac{1}{\sqrt{2}}$. For the first example $N = 64$ and $K = 8$, while for the other two $N = 128$ and $K = 16$. For plotting of images we crop the values to $[0, 1]$, for the material derivative the values are scaled to the interval $[0, 1]$ for plotting, while for the displacement and acceleration plots hue refers to the direction and the intensity is proportional to its norm as indicated by the color wheel.

Fig. 2 shows a first test case. As key frames we consider three images showing two dimensional gaussian distribution with small variance at different positions and of different mass. Spline interpolation is compared with piecewise geodesic interpolation. Furthermore, it is depicted that for the metamorphosis spline, the curve in (x, y, m) -space (position, mass) corresponds almost perfectly to the cubic spline interpolation of the parameters of the Gaussian distribution on the key frames.

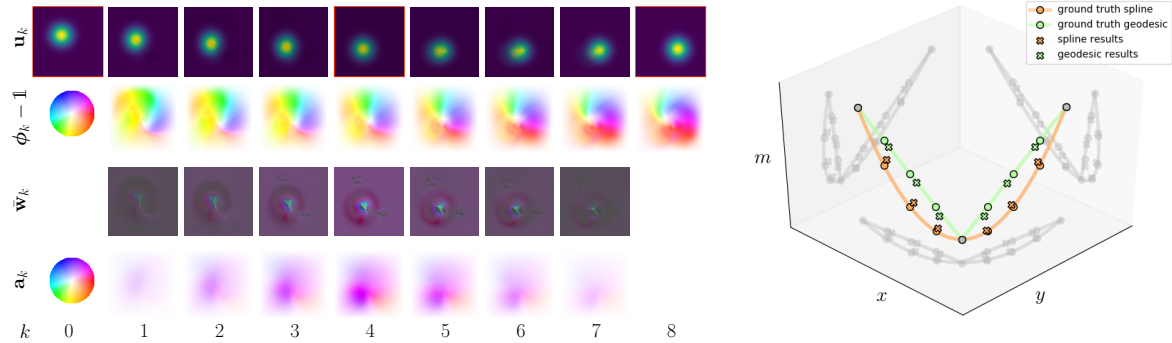


Figure 2: Left: Time discrete spline with framed key frame images (first row), color-coded displacement field (second row), discrete second order material derivative (third row) and color-coded discrete acceleration field (fourth row) for the gaussians example and values of the parameters $\delta = 5 \cdot 10^{-3}$, $\sigma = 1$, $\theta = 5 \cdot 10^{-5}$, $N = 64$. The colors and their intensities indicate the direction and the intensity of the field, as indicated by the color wheel on the left. Right: Euclidean splines in (x, y, m) coordinates for the input parameters versus splines for metamorphosis in (x, y, m) extracted from the numerical results in post-processing, with (x, y) denoting the center of mass and m the mass of the distribution.

As a next step, we conceptually compare splines for metamorphosis and piecewise geodesic paths in Fig. 3. For this specific example, we considered the image of a circle and two identical squares as key frames. The influence of the circle's curvature on the spline segment between the two identical squares is still visible via concave 'edges', while for the piecewise geodesic interpolation any memory of the circle is lost between the squares.

Next, we consider spline interpolation between three human portraits on Fig. 4. The plots of second material derivative and acceleration show a strong concentration around the key frames, where the spline is expected to be smooth and the piecewise geodesic path just Lipschitz.

The analogous observations hold for Fig. 5.

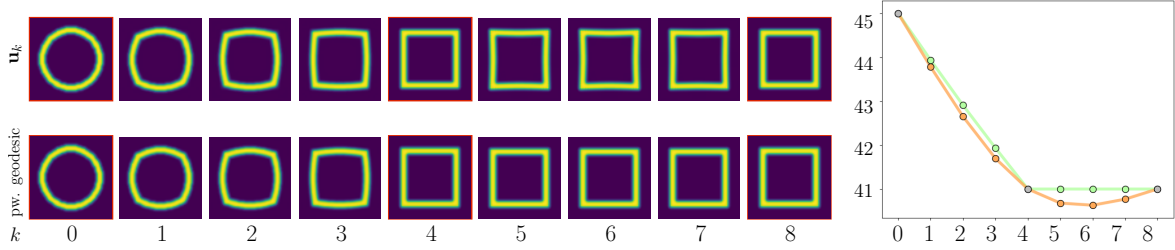


Figure 3: Left: Time discrete spline (top row) and piecewise geodesic (bottom row) interpolation with framed key frames. Right: Width of the interpolated shape measured at the horizontal axis of symmetry (in number of pixels) for a spline interpolation (orange) and piecewise geodesic interpolation (green) showing the concavities ($K = 8$, $\delta = 5 \cdot 10^{-3}$, $\sigma = 1$, $\theta = 5 \cdot 10^{-4}$).

A comparison of splines and piecewise geodesic paths is shown in Fig. 6. One particularly observes that for the faces the shown spline image is thicker and for the letters the spline image shows more round contours than the for the piecewise geodesic counterpart. This is again the non-local impact of key frames beyond those bounding the current interpolation.

Next, we ask for a reconstruction of frames given certain frames at selected time stamps extracted from a video. Here, we compare the resulting spline interpolation and the piecewise geodesic interpolation directly with corresponding frames of the original video as a benchmark for both approaches. Indeed, Fig. 7 shows this comparison of the original frames, spline interpolation and piecewise geodesic interpolation for the images extracted from a video made by David Rogers from Vanderbilt University in the 1950s, which shows the interaction between white blood cells and bacteria. The spline interpolation clearly shows less blending artifacts in comparison to the piecewise geodesic interpolation.

Acknowledgements This work was partially supported by the Deutsche Forschungsgemeinschaft (DFG, German Research Foundation) via project 211504053 - Collaborative Research Center 1060 and project 390685813 - Hausdorff Center for Mathematics.

References

- [BER15] Benjamin Berkels, Alexander Effland, and Martin Rumpf. Time discrete geodesic paths in the space of images. *SIAM J. Imaging Sci.*, 8(3):1457–1488, 2015.
- [BGV19] Jean-David Benamou, Thomas O Gallouët, and François-Xavier Vialard. Second-order models for optimal transport and cubic splines on the Wasserstein space. *Found. Comput. Math.*, 19(5):1113–1143, 2019.
- [BHS05] Bogdan Bojarski, Piotr Hajłasz, and Paweł Strzelecki. Sard’s theorem for mappings in Hölder and Sobolev spaces. *Manuscripta Math.*, 118(3):383–397, 2005.
- [BMTY05] M. Faisal Beg, Michael I. Miller, Alain Trounev, and Laurent Younes. Computing large deformation metric mappings via geodesic flows of diffeomorphisms. *Int. J. Comput. Vis.*, 61(2):139–157, 2005.
- [BV17] Martins Bruveris and François-Xavier Vialard. On completeness of groups of diffeomorphisms. *Journal of the European Mathematical Society*, 19(5):1507–1544, 2017.

- [CCG18] Yongxin Chen, Giovanni Conforti, and Tryphon T Georgiou. Measure-valued spline curves: An optimal transport viewpoint. *SIAM J. Numer. Anal.*, 50(6):5947–5968, 2018.
- [CCLG⁺21] Sinho Chewi, Julien Clancy, Thibaut Le Gouic, Philippe Rigollet, George Stepaniants, and Austin Stromme. Fast and smooth interpolation on Wasserstein space. In *International Conference on Artificial Intelligence and Statistics*, pages 3061–3069. PMLR, 2021.
- [CCT18] N. Charon, B. Charlier, and A. Trouvé. Metamorphoses of functional shapes in Sobolev spaces. *Found. Comput. Math.*, 18(6):1535–1596, 2018.
- [Cia88] Philippe G. Ciarlet. *Mathematical elasticity. Vol. I*, volume 20 of *Studies in Mathematics and its Applications*. North-Holland Publishing Co., Amsterdam, 1988.
- [dB63] Carl de Boor. Best approximation properties of spline functions of odd degree. *J. Math. Mech.*, 12:747–749, 1963.
- [DGM98] Paul Dupuis, Ulf Grenander, and Michael I. Miller. Variational problems on flows of diffeomorphisms for image matching. *Quart. Appl. Math.*, 56(3):587–600, 1998.
- [EKP⁺21] Alexander Effland, Erich Kobler, Thomas Pock, Marko Rajković, and Martin Rumpf. Image morphing in deep feature spaces: Theory and applications. *J. Math. Imaging Vis.*, 63(2):309–327, 2021.
- [ENR20] Alexander Effland, Sebastian Neumayer, and Martin Rumpf. Convergence of the time discrete metamorphosis model on Hadamard manifolds. *SIAM J. Imaging Sci.*, 13(2):557–588, 2020.
- [Fio17] Renato Fiorenza. *Hölder and locally Hölder Continuous Functions, and Open Sets of Class $C^k, C^{k,\lambda}$* . Birkhäuser, 2017.
- [HRW18] Behrend Heeren, Martin Rumpf, and Benedikt Wirth. Variational time discretization of Riemannian splines. *IMA J. Numer. Anal.*, 39(1):61–104, 2018.
- [IKT13] H. Inci, T. Kappeler, and P. Topalov. On the regularity of the composition of diffeomorphisms. *Mem. Amer. Math. Soc.*, 226(1062):vi+60, 2013.
- [JM00] Sarang C. Joshi and Michael I. Miller. Landmark matching via large deformation diffeomorphisms. *IEEE Trans. Image Process.*, 9(8):1357–1370, 2000.
- [JRR21] Jorge Justiniano, Marko Rajković, and Martin Rumpf. Splines for Image Metamorphosis. In *Scale Space and Variational Methods in Computer Vision: 8th International Conference, SSVM 2021, Virtual Event, May 16–20, 2021, Proceedings*, pages 463–475. Springer International Publishing, 2021.
- [Mos69] Umberto Mosco. Convergence of convex sets and of solutions of variational inequalities. *Advances in Math.*, 3:510–585, 1969.
- [MTY02] Michael I. Miller, Alain Trouvé, and Laurent Younes. On the metrics and Euler-Lagrange equations of computational anatomy. *Annu. Rev. Biomed. Eng.*, 4(1):375–405, 2002.
- [MY01] Michael I. Miller and Laurent Younes. Group actions, homeomorphisms, and matching: a general framework. *Int. J. Comput. Vis.*, 41(1–2):61–84, 2001.
- [NHP89] Lyle Noakes, Greg Heinzinger, and Brad Paden. Cubic splines on curved spaces. *IMA J. Math. Control Inform.*, 6(4):465–473, 1989.

- [Nir66] Louis Nirenberg. An extended interpolation inequality. *Ann. Scuola Norm. Sup. Pisa Cl. Sci. (3)*, 20:733–737, 1966.
- [NŠ91] Jindřich Nečas and Miroslav Šilhavý. Multipolar viscous fluids. *Quart. Appl. Math.*, 49(2):247–265, 1991.
- [PS16] Thomas Pock and Shoham Sabach. Inertial proximal alternating linearized minimization (iPALM) for nonconvex and nonsmooth problems. *SIAM J. Imaging Sci.*, 9(4):1756–1787, 2016.
- [RY13] Casey L. Richardson and Laurent Younes. Computing metamorphoses between discrete measures. *J. Geom. Mech.*, 5(1):131–150, 2013.
- [RY16] Casey L. Richardson and Laurent Younes. Metamorphosis of images in reproducing kernel Hilbert spaces. *Adv. Comput. Math.*, 42(3):573–603, 2016.
- [SVN15] Nikhil Singh, François-Xavier Vialard, and Marc Niethammer. Splines for diffeomorphisms. *Med. Image Anal.*, 25(1):56–71, 2015.
- [TV12] Alain Trouvé and François-Xavier Vialard. Shape splines and stochastic shape evolutions: a second order point of view. *Quart. Appl. Math.*, 70(2):219–251, 2012.
- [TV19] Rabah Tahraoui and François-Xavier Vialard. Minimizing acceleration on the group of diffeomorphisms and its relaxation. *ESAIM Control Optim. Calc. Var.*, 25, 2019.
- [TY05a] Alain Trouvé and Laurent Younes. Local geometry of deformable templates. *SIAM J. Math. Anal.*, 37(1):17–59, 2005.
- [TY05b] Alain Trouvé and Laurent Younes. Metamorphoses through Lie group action. *Found. Comput. Math.*, 5(2):173–198, 2005.
- [Via20] François-Xavier Vialard. Variational second-order interpolation on the group of diffeomorphisms with a right-invariant metric. In *Mathematics Of Shapes And Applications*, pages 1–14. World Scientific, 2020.
- [You10] Laurent Younes. *Shapes and diffeomorphisms*, volume 171 of *Applied Mathematical Sciences*. Springer-Verlag, Berlin, 2010.

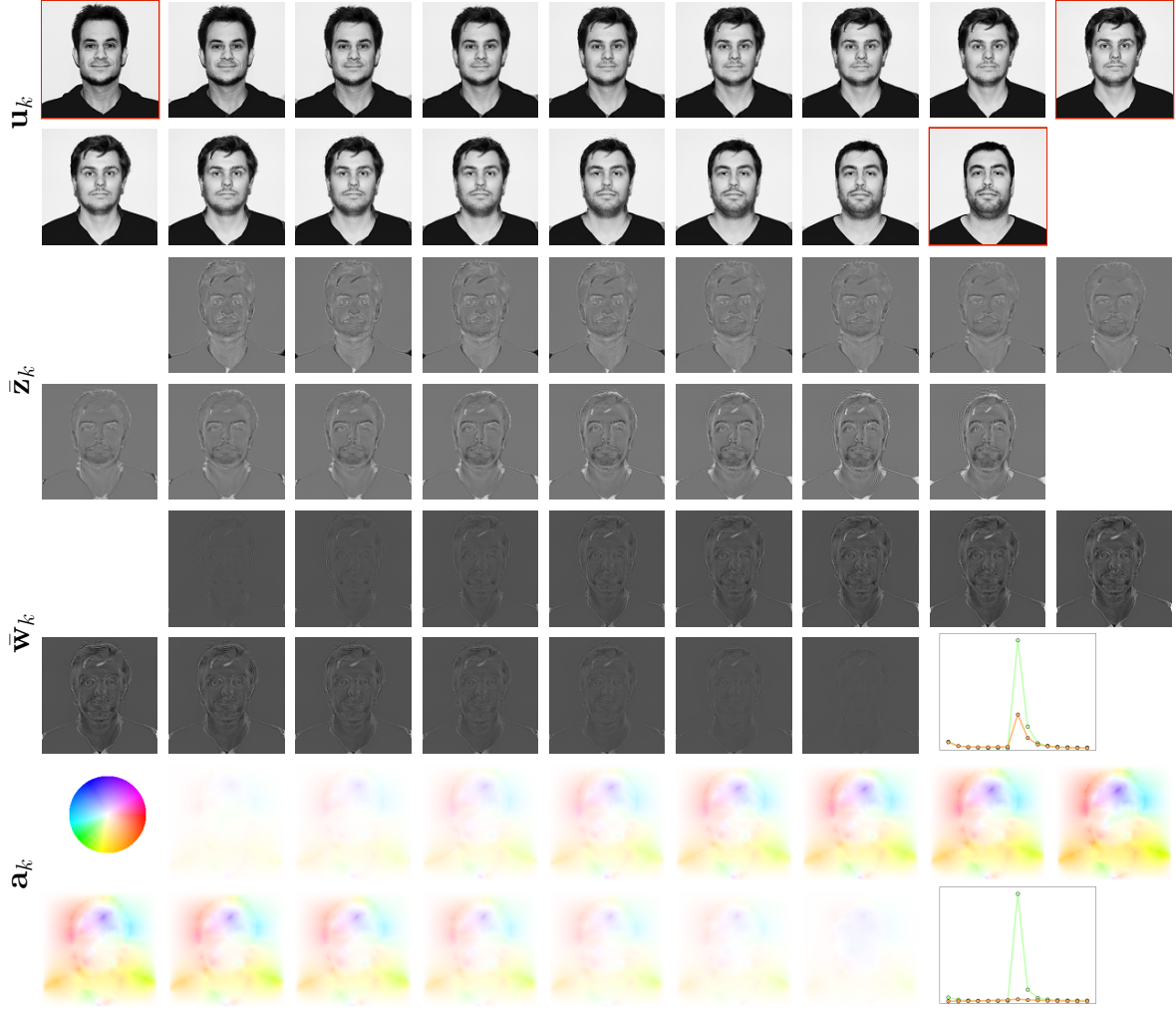


Figure 4: Time discrete spline with framed fixed images (first and second row), first order material derivative slack variable $\bar{\mathbf{z}}$ (third and fourth row), second order material derivative with energies comparison (fifth and sixth row) and color-coded acceleration field with energies comparison (seventh and eighth row) for values of the parameters $\delta = 2 \cdot 10^{-2}$, $\sigma = 2$, $\theta = 8 \cdot 10^{-4}$. The graphics on the right in row four and six show for the spline (orange) time plots of the L^2 -norm of the actual second order material derivative $\hat{\mathbf{w}}$ and the dissipation energy density reflecting motion acceleration, respectively. This is compared to the corresponding piecewise geodesic interpolation (green) (not visualized here, cf. Fig. 6).



Figure 5: Left: Time discrete spline with framed fixed images (top and bottom row). Right: Energy density norm of acceleration flow $\|W_A(\nabla_{MN}\mathbf{a}_k)\|_{L^1_{MN}}$ (top), and L^2 -norm of the actual second order material derivative $\hat{\mathbf{w}}$ (bottom). Parameter values: $\delta = 10^{-3}$, $\sigma = 2$, $\theta = 2 \cdot 10^{-5}$.

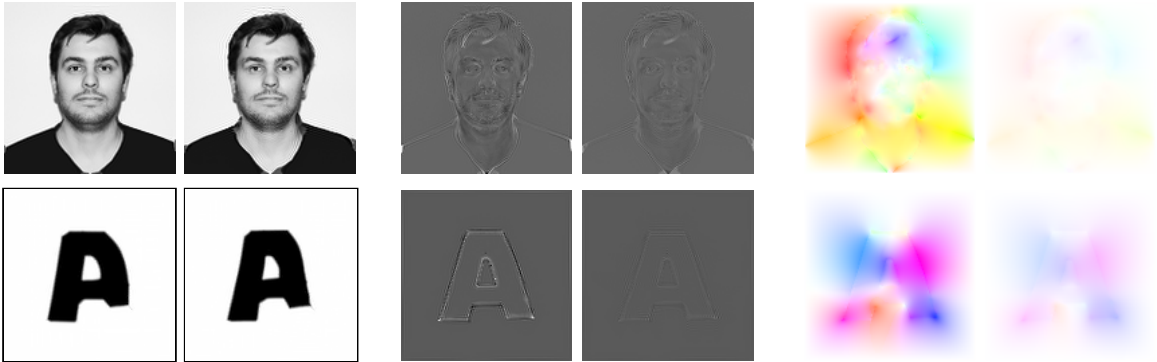


Figure 6: Top row: Image \mathbf{u}_{11} for the human face example, second order material derivative $\hat{\mathbf{w}}_k$ and acceleration field \mathbf{a}_k for $k = 8$, for the time discrete piecewise geodesic (left image of each panel pair) and spline (right image of each panel). The pairs of material derivatives and the acceleration fields are jointly scaled to reflect the differences in intensities. Bottom row: Same visualization of image \mathbf{u}_4 from the letter example.

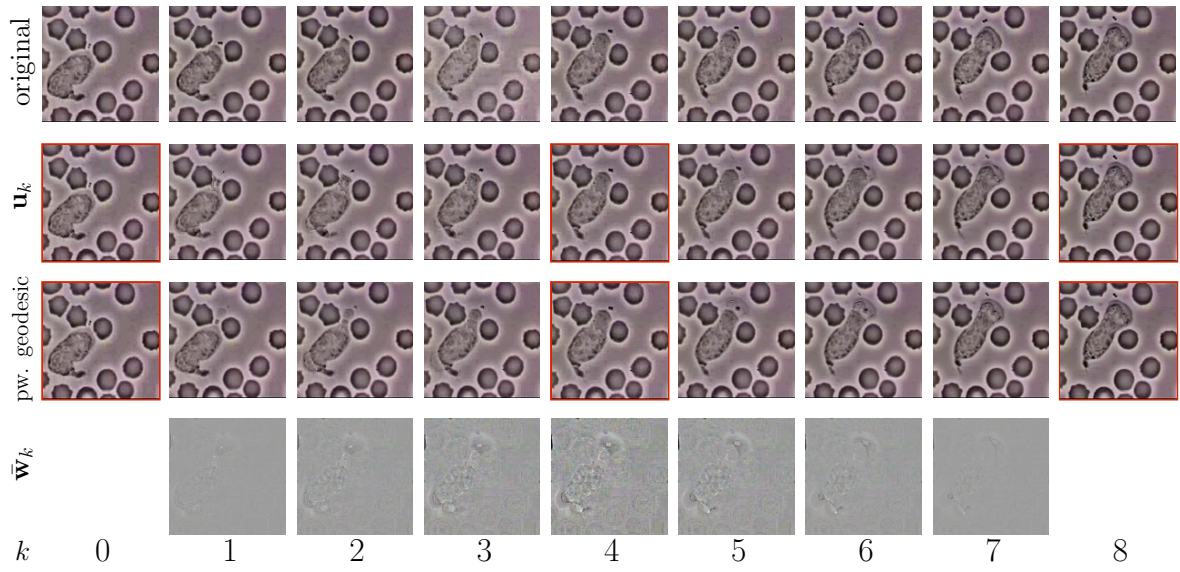


Figure 7: First row: The original frames extracted from the video showing white blood cell (neutrophil) chasing a *Staphylococcus aureus* bacterium. The images are courtesy of Robert A. Freitas, Institute for Molecular Manufacturing, California, USA. Second row: Time discrete spline with framed fixed images. Third row: Time discrete piecewise geodesic with framed fixed images. Fourth row: Fully discrete second order material derivative for the discrete spline interpolation. The values of parameters are $\delta = 4 \cdot 10^{-2}$, $\sigma = 2.5$, $\theta = 1.6 \cdot 10^{-4}$.